

Ionic Liquids and Organic Ionic Plastic Crystals: Advanced Electrolytes for Safer High Performance Sodium Energy Storage Technologies

Andrew Basile,* Matthias Hilder, Faezeh Makhlooghiazad, Cristina Pozo-Gonzalo, Douglas R. MacFarlane, Patrick C. Howlett, and Maria Forsyth*

Electrolytes composed entirely of salts, namely, ionic liquid solvents paired with a target ion salt, have been studied extensively within lithium batteries and have recently garnered interest as advanced electrolytes for sodium chemistries. In this review, the unique properties of ionic liquid electrolytes and their solid-state analogs, organic ionic plastic crystals, are examined. Structure–property relationships, the effect of salt addition, cation and anion functionalization, and their effect upon physicochemical and thermal character are discussed. The authors discuss the use of ionic liquid electrolytes paired with organic solvents (referred to as hybrids) and briefly present the impact of using water as an additive. The majority of the literature presented herein covers studies of sodium electrolytes at Na^+ concentrations greater than 50 mol%, labelled as superconcentrated electrolytes, which have recently been investigated for their beneficial device performance and improved target ion mobility. The developing research of ionic liquids toward the oxygen reduction reaction is also presented toward the realization of Na-O_2 chemistries to rival that of conventional Li-ion; gaining fundamental understanding of the active species during discharge, its resultant nucleation and character. Additionally, the properties of the electrode–electrolyte interface resulting from the interaction between typical sodium anodes with ionic liquid electrolytes are discussed.

1. Importance and Motivation for Advanced Electrolytes

Researchers around the globe are currently on a resolute undertaking to develop the new technologies that can help us to power our modern way of life in a cheap and sustainable manner.^[1] Chief among these technologies are the batteries which currently provide energy storage solutions in a diverse array of modern devices;^[2] powering portable electronics,

computers and power tools, and emergent energy storage solutions for transport or for storing renewable energy in an ever-evolving ‘smart grid’. Each of these products requires diverse battery technologies, with many batteries well-suited for specific cases, e.g., Li-ion batteries for the electrification of vehicles due to their light weight and therefore intrinsic energy density (typically 100–265 Wh kg^{-1}). In fact, the adoption and penetration of electric vehicles (EVs) in the transport market is quickly becoming synonymous with battery research, with advanced lithium technologies such as lithium–sulfur (Li–S) and lithium–oxygen (Li– O_2) envisaged as the next generation of batteries to power our vehicles (theoretical energy densities of 2567 and 3505 Wh kg^{-1} respectively).^[3]

Lithium technologies power many of our modern devices and so are well understood, however sodium chemistries share commonalities. They are also well known because both Li and Na batteries were investigated in tandem near the end of the last century prior to the commercialization of Li-ion by Sony.^[2,4] In fact, Sodium

battery energy storage systems (ESS) precede Li-ion, with the description of a $\beta\text{-Al}_2\text{O}_3$ Na^+ ion conducting solid electrolyte in the 1960s by Kummer and Weber of Ford Motor Co which enabled sodium/sulfur technologies.^[5] Since then, sodium technologies have found use in stationary applications and usually consist of one of two battery technologies, these are Na–S and zero emission battery research activities.^[6]

Both these cell chemistries require operation at elevated temperatures ($\approx 300^\circ\text{C}$) which enables the use of a molten sodium

Dr. A. Basile, Dr. M. Hilder, Dr. F. Makhlooghiazad, Dr. C. Pozo-Gonzalo, Prof P. C. Howlett, Prof. M. Forsyth
Institute for Frontier Materials (IFM)
Deakin University
Burwood, Victoria 3125, Australia
E-mail: andrew.basile@deakin.edu.au; maria.forsyth@deakin.edu.au

The ORCID identification number(s) for the author(s) of this article can be found under <https://doi.org/10.1002/aenm.201703491>.

Dr. C. Pozo-Gonzalo, Prof P. C. Howlett, Prof. M. Forsyth
Australian Centre for Electromaterials Science (ACES) Deakin University
Burwood, Victoria 3125, Australia

Prof. D. R. MacFarlane
Australian Centre for Electromaterials Science (ACES)
School of Chemistry
Monash University
Clayton, Victoria 3800, Australia

DOI: 10.1002/aenm.201703491

anode and molten S/NiCl_2 cathode. These high temperatures also improve the ionic conductivity of the solid sodium $\beta\text{-Al}_2\text{O}_3$ ceramic electrolyte and prevent the formation of metallic dendrites. Since this time many installations have been made by NGK Insulators Japan for load-levelling applications using Na–S cells ($150\text{--}240\text{ Wh kg}^{-1}$)^[7] in $200\text{ kW}/1.2\text{ MWh}$ units with the last count at installations totaling 450 MW as of 2013 in a U.S. Department of Energy Grid energy Storage report (U.S. DOE),^[8] and current estimates expected to be closer to $530\text{ MW}/3.7\text{ GWh}$.^[9] Within that U.S DOE report it is recognized that new chemistries will be required to meet the future requirements of cost competitive energy storage technologies. In a second report in 2014 the U.S. DOE followed up with an Energy Storage Safety Strategic Plan which specifically targeted the second key challenge set forth regarding the validation of safety and reliability within future energy storage technologies.^[10] This is especially important as the number of battery ESS begins to increase (largest Li-ion ESS: $100\text{ MW}/129\text{ MWh}$ in South Australia to support power grid) as the targeted battery price $<\$100\text{ kWh}^{-1}$ progressively becomes a reality ahead of expectations^[11]

In order to increase the safety of these sodium based batteries, a simple solution is to decrease the operating temperature, as achieved with common Li-ion cells. A startup named Tiamat has recently begun to design and develop a technology unveiled by a French consortium, a Na-ion device in 18650 format claiming 90 Wh kg^{-1} and 2000 cycles.^[12] Work has also been carried out by Faradion who have reported >400 cycles of a hard carbon layered oxide cell with 100% depth of discharge to 80% of capacity at rates between $\text{C}/10$ to $\text{C}/2$.^[13] These cells display energy densities similar to those of their Li-ion counterparts from a decade ago, thus there is still room for improvement to reach the values envisaged to power our future energy-hungry society. The use of sodium metal in a device will allow for this advancement in capacity, where Na-O_2 can achieve 1605 Wh kg^{-1} .^[14] However utilizing energy dense Na metal brings about additional safety concerns, analogous to Li metal anodes, such as heterogeneous metal deposition during plating, dendritic growth, the low melting point of sodium metal, and electrolyte decomposition due the highly reducing environment of an alkali metal anode. This is typical when using the conventional organic electrolytes, grandfathered into alkali metal technologies because of their success and compatibility with Li-ion electrodes. However, since the report of highly efficient and stable lithium deposition from an ionic liquid electrolyte, this field of electrolyte development has seen increased research.^[15]

Novel electrolytes such as ionic liquids (ILs) which themselves can have low reactivity have proven well suited for this task. Sodium metal anodes, and Li alike, can be plated and stripped with high efficiency when using these ionic liquids.^[16] The prohibitive expense of ionic liquids has been a deterrent to their uptake in Li technologies, however by moving to Na technologies the costs of cells will drop significantly due to the accessibility of elemental sodium and the ability to use Al instead of Cu as the current collector. Thus, advanced electrolytes such as ionic liquids and organic ionic plastic crystals (OIPCs) may ultimately find their way into Na-ion technologies as part of a holistic approach to revitalize the technology, much like the novelty of $\beta\text{-Al}_2\text{O}_3$ electrolytes brought about high temperature Na–S.



Andrew Basile received his formal training in nanotechnology at RMIT University (Australia) before receiving his Ph.D. in 2014 with the Commonwealth Scientific and Industrial Research Organization (CSIRO Australia). His Ph.D. research covered the characterization of solid–

electrolyte interphases on lithium metal from ionic liquid electrolytes. Following on from postdoctoral research at the University of Warwick (United Kingdom) on the topic of nanoscale electrochemical imaging techniques, his current research as an Alfred Deakin Fellow at Deakin University is focused on the design and development of surface engineered SEI layers on sodium metal anodes for advanced energy storage technologies.



Patrick C. Howlett received his Ph.D. from Monash University in collaboration with CSIRO in 2004. His research relates to electrochemical devices and surface engineering through the manipulation of electrode interphases using novel materials approaches. He is currently co-director of the Battery Technology Research

Innovation Hub (BatTRI-Hub) at Deakin University, focused on advanced battery prototyping and translating technologies from lab to industry. His research covers ionic liquids, polymer electrolytes, plastic crystal electrolytes as well as their composites and reactive metals such as lithium and sodium.



Maria Forsyth is an Australian Laureate Fellow and Alfred Deakin Professorial Fellow, elected to the Australian Academy of Sciences in 2015. She is Associate Director of the ARC Centre of Excellence in Electromaterials Science (ACES), leading the research effort in energy storage and corrosion science at Deakin University in Australia.

Specifically, her work has focused on understanding the phenomenon of charge transport at metal/electrolyte interfaces within novel electrolytes, including, ionic liquids, polymer electrolytes, and plastic crystals.

Table 1. Structure and abbreviations of common ionic liquid cations/anions in use for sodium battery electrolyte research.

Ion	Abbreviation	Structure
Quaternary cations		
Alkylmethylimidazolium	[Cnmim] ⁺	
Alkylmethylpyrrolidinium	[Cnmpyr] ⁺	
Ammonium (ether functionalized)	[N _{n,n,n,n,O}] ⁺ a)	
Ammonium	[N _{n,n,n,n}] ⁺	
Phosphonium	[P _{n,n,n,n}] ⁺	
Spirocyclic ammonium	ASX _(n,n) ⁺	
Anions		
Bis(fluorosulfonyl)imide ^{b)}	[FSI] ⁻	
Bis(trifluoromethanesulfonyl)imide ^{b)}	[TFSI] ⁻	
Dicyanamide	[DCA] ⁻	
Hexafluorophosphate	[PF ₆] ⁻	
Tetrafluoroborate	[BF ₄] ⁻	

^{a)}The O represents an ether oxygen, not to be confused with zero (0); ^{b)}These anions are classed as "imides" to avoid confusion with the literature, rather than the correct nomenclature "amides."

Ionic liquids are novel solvents that possess an abundance of unique properties compared to conventional electrolytes. The majority of these solvents are composed of organic salts with bulky asymmetric structures. They are capable of dissolving a wide range of metal salts up to high concentration. In addition, they are considered as "safer" electrolytes as they themselves have low flammability due to being virtually nonvolatile. Thus, ILs have found themselves used as battery electrolyte additives in the form of fire-retardants.^[17] Ionic liquids have an intrinsic ionic conductivity, being composed entirely of ions, and exhibit wide electrochemical stability—a prerequisite for high voltage battery electrolytes. Due to the enormous amount of possible anion and cation pairings, the properties of an IL can vary accordingly as a function of the material's chemistry. As such, ILs have found application in a variety of fields, and the reader is directed to comprehensive reviews covering the properties and applications of ionic liquids.^[18–24] A list outlining several cations and anions covered within this review can be found in **Table 1**. It should be noted however that ILs do not only possess intrinsic properties to the benefit of battery technologies, they are also highly viscous in most cases, suffer from lower molar conductivity at low temperatures in comparison with conventional organic electrolytes (especially near T_m) and typically consist of highly fluorinated anions such as the [FSI]⁻ and [TFSI]⁻ species.

In order to develop these advanced Na battery technologies, it is essential to gain an understanding of the fundamental chemistry which occurs upon addition of a Na salt to an ionic liquid to predict its speciation and interactions with the bulk solvent. These factors will affect the ion transport of the charge carrier, as well as dictate the interactions at an electrode interface. It is also possible to tailor the design of ionic liquids, through modifying the anion or cation functionality (e.g., cyano, fluoro, alkoxy functionality), to define the electrolyte properties. This can also be made possible through the use of additives (i.e., H₂O, vinylene carbonate) which have been used routinely in conventional battery electrolytes in the past.^[25,26] In addition to the intrinsic bulk properties of the electrolyte, an important role of the IL is the promotion of a beneficial solid–electrolyte interphase (SEI).^[27–30] This SEI often dictates the electrochemical stability, ion/charge transport at the electrode surface and may be the critical factor in the successful cycling of an

electrode.^[31–33] The unique interfacial and bulk structuring of these electrolytes are also of particular interest when it comes to controlling electrochemical reactions at an electrode–electrolyte interface.^[34–37]

There are many reviews in the literature covering specific applications including in electrochemical devices^[21] such as Li battery electrolytes,^[19,21,38] fuel cells^[19] and solar cells^[39] to media useful for CO₂ capture,^[40] metal electrodeposition^[41] and chemical synthesis.^[23,42] Under the umbrella of the term ionic liquids, one can also loosely include other forms of electrolytes such as deep eutectic solvents (DESS),^[43] solvate ionic liquids,^[19] and polymerized ionic liquids (PILs).^[44,45] More recently super concentrated electrolyte systems where the lithium or sodium ion concentration can exceed 3 M—including those based on organic solvents^[46–48] as well as ionic liquids,^[49–52] have shown promise for cycling of both lithium and sodium metal anodes. Solid state analogues of ionic liquids include gelled ionic liquids^[53] as well as organic ionic plastic crystals.^[54] It is worth noting that the properties of the resultant IL solvent/electrolyte system is crucially dependent upon the functionality designed into the cation–anion IL pair for a target application.

In the field of Na batteries, ionic liquids remain quite novel. Their compatibility in Na-ion technologies against hard carbon materials has been reported^[55,56] as well as against Na metal anodes.^[57–59] Currently, only a small fraction of a percent of global ESS is supplied by batteries (Pb-acid), while the lion's share of 95% is via inflexible pumped-hydro energy storage (>100 GW). Thus, cheap and flexible sodium technologies are inherently well suited for stationary ESS, due to their elemental abundance and greater mass. Hence, they are envisioned as grid ESS or “behind-the-meter” home storage as enabling technologies which will not generate electricity but will enable critical advances to modernize the power grid.^[60]

In this review we focus on the state-of-the-art battery technologies comprised of an ionic liquid electrolyte for sodium energy storage, or, their solid-state cousins organic ionic plastic crystals. The physicochemical and transport properties of these novel ionic electrolytes, both in liquid and solid state and their electrochemical performance with different cell chemistries using a variety of electrode materials will also be discussed. Recent studies on the topic of hybrid electrolytes, and electrolytes to support the oxygen reduction reaction with insight on their discharge products are also included. Finally, the electrode–electrolyte interface which governs much of a cell's performance is also included for the small body of work which already exists in this area.

2. Novel Physicochemical Properties for Na Energy Storage

This section focuses on the physicochemical and electrochemical properties of ionic liquid electrolytes for sodium battery devices, with the main focus being on ionic liquids and their sodium salt solutions. **Table 2** summarizes a range of ILs and compositions found in the literature including the glass transition,^[61] melting and decomposition temperatures (T_g , T_m , T_d , respectively) and conductivity, σ , viscosity, η , and density, ρ .^[62] For brevity, the table lists the highest concentration reported

for each particular study. For an exhaustive list of all reported concentrations we have prepared larger tables within the Supporting Information; these tabulated values were extracted from figure data using WebPlotDigitizer (Automeris LLC) when accurate values were not provided. In addition to these electrolyte properties, parameters reported from key device studies with ionic liquid electrolytes are also presented in the following section **Table 3**. We also briefly discuss and compare tertiary systems which highlight the effect of additives such as molecular organic solvents^[63,64] and water.^[65] Polymer or gel electrolytes which are typically prepared by solvent casting or electrospinning typically include polyvinylidene fluoride (PVdF),^[66–69] polyethylene oxide (PEO), or poly(ethylene)glycol dimethyl ether (PEGDME),^[70–73] however they are not discussed herein.^[53,63]

2.1. Thermal Properties

The operational temperature window of a device is often determined by the thermal properties of the electrolyte. Typically, the upper temperature limit is defined by the evaporation temperature or decomposition temperature of the electrolyte, with evaporation being a major limitation of traditional organic solvent based electrolytes. In general, device performance is best above the glass transition temperature or the melting point where mobility is highest (i.e., in the liquid state). Classical organic solvent electrolytes are often based on dimethylcarbonate which has a relatively low boiling point of 90 °C. Due to the electrostatic interactions between the ions in ionic liquids, ionic liquids typically do not evaporate and thus their upper limit is usually determined by their decomposition temperature.

Thermogravimetric analysis (TGA) of sodium solutions of pyrrolidinium, and phosphonium ionic liquids has determined the decomposition temperature to typically be above 300 °C. For instance, a solution of NaTFSI salt in *N*-methyl-*N*-butylpyrrolidinium bis(trifluoromethanesulfonyl)imide (NaTFSI/C₄mpyr[TFSI]) at 400 °C. Two studies reported the decomposition temperatures of C₄mpyr[TFSI] systems with different solutes (NaBF₄, NaPF₆, NaClO₄, NaDCA, NaTFSI) which ranged from 330 to 360 °C suggesting that the nature of the added salt had little effect,^[59,74] with the exception of NaPF₆ which decomposed near 100 °C.^[74] Surprisingly, ionic liquid solutions based on bis(fluorosulfonyl)imide ([FSI][−] anion) and the ammonium cation such as trimethyl-hexylammonium, dibutyl-dimethylammonium or 5-azoniaspiro[4.4]nonane (N₁₁₁₆[FSI], N₁₁₄₄[FSI], ASN_(4,4)[FSI] respectively) were reported to possess a much lower thermal stability (177 °C),^[75] although our own observations suggest that these low temperature limits can be the result of water (or other) impurities which appear to catalyze the decomposition process in FSI based ILs. Regardless, IL electrolytes are considered as superior to solvent based electrolytes in terms of their upper temperature limit. One caveat that is important to consider is the fact that TGA is a dynamic technique and hence the true thermal stability under static conditions may be considerably lower than the reported values.^[76]

Dissolving a salt in a liquid usually results in a lower melting point (melting point depression), however, with salt addition the viscosity of the system also increases, which leads to a

Table 2. Thermal and physicochemical properties of ionic liquid electrolytes at their highest reported concentration of Na⁺ salt for each study. An exhaustive list of each concentration can be found within the Supporting Information.

[Salt]/ionic liquid	Phase transitions [°C]				Physicochemical properties at given temperature				Reference
	t_{Na^+}	T_g	T_m	T_d	σ [mS cm ⁻¹]	η [mPa s]	ρ [g cm ⁻³]	T [°C]	
Ammonium cation									
90 mol% NaFSI/N ₁₁₄₄ [FSI]	–	–21	60	197	0.7	356	–	25	[75]
90 mol% NaFSI/N ₁₁₁₆ [FSI]	–	–25	57	197	0.3	416	–	25	[75]
59 mol% NaTFSI/N ₂₍₂₀₂₀₁₎₃ [TFSI]	–	–19	–	–	0.016	838	1.450	60	[82]
55 mol% NaFSI/N ₂₍₂₀₂₀₁₎₃ [FSI]	–	–45	–	–	0.0027	791	1.445	20	[181]
Imidazolium cation									
90 mol% NaFSI/C ₂ mim[FSI]	–	–57.0	29	–	1.2	144	1.660	25	[79]
30 mol% NaTFSI/C ₂ mim[TFSI]	–	–74.4	–	–	2.5	–	–	25	[77]
20 mol% NaTFSI/C ₄ mim[TFSI]	–	–75.8	–	–	1.3	–	–	25	[77]
30 mol% NaTFSI/C ₂ mim[TFSI]	–	–	–	–	2.4	127	–	20	[89]
50 mol% NaFSI/ C ₂ mim[FSI]	0.35	–	–	–	5.9	–	–	90	[51]
50 mol% NaAlCl ₄ /C ₂ mimAlCl ₄	–	–	–	–	5.5	–	–	25	[94]
50 mol% NaAlCl ₄ /C ₂ mimFeCl ₄	–	–	–	–	6.0	–	–	25	[94]
0.75 M NaBF ₄ /C ₂ mim[BF ₄]	–	–	–	380	8.0	–	–	20	[182]
3.8 mol% NaBF ₄ /C ₄ mim[BF ₄]	–	–	–	–	3.2	130	1.212	25	[183]
Phosphonium cation									
42 mol% NaFSI/P ₁₁₁₁₄ [FSI]	0.33	–71	6	305	0.9	567	1.497	20	[95]
20 mol% NaPF ₆ /P ₁₁₄₁₄₁₄ [FSI]	0.19	–	47	–	0.06	–	–	20	[98]
20 mol% NaFSI/P ₁₁₄₁₄₁₄ [FSI]	0.37	–	9	–	0.6	–	–	20	[98]
20 mol% NaTFSI/P ₁₁₄₁₄₁₄ [FSI]	0.31	–73	–	–	0.4	–	–	20	[98]
45 mol% NaPF ₆ /P ₁₁₄₁₄₁₄ [FSI]	–	–73	–	–	0.5	–	–	20	[58]
80 mol% NaTFSI/P ₁₁₁₁₄ TFSI	–	–	217	–	0.0003	–	–	20	[180]
80 mol% NaFSI/P ₁₁₄₄₄ FSI	–	–	107	–	0.27	–	–	20	[180]
80 mol% NaTFSI/P ₁₁₄₄₄ TFSI	–	–	256.4	–	0.0002	–	–	20	[180]
45 mol% NaFSI/P ₁₁₄₁₄₁₄ [FSI]	0.35	–78	–	–	0.5	–	–	20	[181]
Pyrrolidinium cation									
1 M NaClO ₄ /C ₄ mpyr[TFSI]	0.2	–	–	360	1.0	213	–	30	[59]
1 M NaBF ₄ /C ₄ mpyr[TFSI]	0.2	–	–	360	1.5	285	–	30	[59]
1 M NaDCA/C ₄ mpyr[TFSI]	0.2	–	–	360	0.5	425	–	30	[59]
1 M NaPF ₆ /C ₄ mpyr[TFSI]	0.2	–	–	360	1.0	327	–	30	[59]
20 mol% NaTFSI/C ₄ mpyr[TFSI]	–	–83	–30	–	0.6	–	–	22	[78]
14 mol% NaTFSI/C ₄ mpyr[TFSI]	–	–80	–	–	1.3	188	1.440	25	[80]
0.3 M NaTFSI/C ₄ mpyr[TFSI]	–	–	–	–	1.3	172	–	20	[86]
0.3 M NaTFSI/C ₄ Hpyr[TFSI]	–	–	–	–	1.5	123	–	20	[86]
1 M NaTFSI/C ₄ mpyr[TFSI]	0.25	–	–	400	0.5	–	–	25	[112]
20 mol% NaFSI/C ₃ mpyr[FSI]	–	–	–	–	3.2	312	–	25	[93]
60 mol% NaFSI/C ₃ mpyr[FSI]	–	–	–	–	0.02	794	–	25	[84]
7 mol% NaFSI/C ₃ mpyr[FSI]	–	–101	–9	–	1.0	–	–	20	[81]
1 M NaBF ₄ /C ₄ mpyr[TFSI]	–	–	–	350	1.9	–	–	25	[74]
1 M NaClO ₄ /C ₄ mpyr[TFSI]	–	–	–	350	1.0	–	–	25	[74]
1 M NaTFSI/C ₄ mpyr[TFSI]	–	–	–	350	0.5	–	–	25	[74]
1 M NaPF ₆ /C ₄ mpyr[TFSI]	–	–	–	100	0.4	–	–	25	[74]
55 mol% NaTFSI/C ₄ mpyr[TFSI]	0.11	–80	–	317	0.5	–	–	25	[64]
50 mol% NaFSI/C ₃ mpyr[FSI]	0.32	–	–	–	–	–	–	–	[88]

Table 2. Continued.

[Salt]/ionic liquid	Phase transitions [°C]				Physicochemical properties at given temperature				Reference
	t_{Na^+}	T_g	T_m	T_d	σ [mS cm ⁻¹]	η [mPa s]	ρ [g cm ⁻³]	T [°C]	
Low melting salts									
56 mol% NaFSI/KFSI	–	–	–	–	0.3	5925	2.160	60	[87]
45 mol% NaFSI/KFSI	–	67	–	–	–	–	–	–	[97]
10 mol% NaTFSI/CsTFSI	–	–	–	–	12	42	2.290	150	[96]

higher glass transition temperature, T_g . Typically, a low T_g or T_m means higher ion mobility at a given temperature and therefore low transition temperatures are desirable to achieve low operation temperatures. Indeed, most low sodium content ionic liquids (i.e., <1 M or 25 mol%) show low T_g values (typically –90 to –75 °C). This includes the range of imidazolium and pyrrolidinium TFSI solutions shown in Table 2.^[75,77–80] The lowest T_g reported was for the 7 mol% NaFSI in propyl-methylpyrrolidinium bis(fluorosulfonyl)imide (C₃mpyr[FSI]) electrolyte at –101 °C.^[81] Some high sodium content IL solutions (>25%) also show a low T_g (below –50 °C) and thus are suitable to be used for low temperature applications. These include various imidazolium,^[77,79] pyrrolidinium,^[80] ammonium,^[75,82,83] and phosphonium^[58] ionic solutions with T_g of –80 to –70 °C.

Comparing the reported T_g values suggests that the increase in cation size (e.g., [C₂mim]⁺ vs [C₄mim]⁺) increases T_g . This is possibly caused by the stronger degree of intermolecular interactions.^[77] Comparing the anion effect for [C₂mim]⁺ shows a much lower T_g for the [FSI][–] anion (–91 °C)^[79] as compared to the [TFSI][–] anion (–77 °C),^[77] at the same 20 mol% concentration. Suggesting that there are much stronger interactions in the TFSI electrolyte. A plasticizing effect of the [FSI][–] anion leading to lower T_g has been reported previously.^[73] Also comparing butyl-methyl substituted IL cations indicates that there are less intermolecular interactions in pyrrolidinium TFSI solutions than in the corresponding imidazolium sample which shows a higher T_g ; the glass transition at 20 mol% NaTFSI in C₄mpyr[TFSI] is shown at –83^[78] and –77 °C in C₄mim[TFSI].^[77] Interestingly, for high salt concentration samples, there seems

to be minimal effects of the salt content on T_g in homogeneous solutions.^[75,77,84] In the case of the ether functionalized ammonium cation, *N*-ethyl-2-(2-methoxyethoxy)-*N,N*-bis(2-(2-methoxyethoxy)ethyl)ethan-1-ammonium, the T_g is also lower for the NaFSI containing solutions of 41 mol% NaX/N₂(2O2O1)₃[TFSI] electrolyte (where X = TFSI or FSI, –44 °C vs –53 °C)^[82,83] further highlighting the plasticizing properties of the [FSI][–] anion.

The investigation of combustion and decomposition behavior of many ILs has also been carried out to address the actual fire hazard these novel solvents may pose. Eshetu et al. study the dynamic and isothermal TGA thermal stability, biodegradability and combustion behavior across a range of pyrrolidinium ILs along with an ethylene carbonate (EC): dimethyl carbonate (DMC) comparator.^[85] Aside from demonstrating higher thermal stability of these novel IL solvents over organic carbonates (organics ignite immediately, ILs ignite after ≈5 min of extreme heat), the study reveals that these properties are highly related to the structure of the cation, anion, their functionality (i.e., ether oxygens) and alkyl chain length. The ignition of these ILs followed a similar trend to TGA results, whereby longer alkyl chains provided shorter ignition times in line with T_d . Increasing the chain length also provided more carbon as fuel content during burning, larger heat of combustion and greater CO₂ emissions. In addition to CO₂, combustion releases SO₂, NO, and HF as major products along with soot and aldehydes. Importantly, the flammability of these flame retarding solvents is categorized as being similar to polymer characteristics, due to their thermal decomposition which in turn generates flammable moieties, rather than their vaporization as with organic electrolytes.

Table 3. Performance of various electrode materials within cells comprising ionic liquid electrolytes.

Variables	Electrode	Electrolyte	C_{Dis} [mAh g ⁻¹]	Charging rate		T [°C]	Reference
				C-rate	mA g ⁻¹		
Rate and temperature	NaFePO ₄	1 M NaBF ₄ /C ₄ mpr[TFSI]	152	C/20	–	75	[59]
Rate, concentration, and temperature	NaCrO ₂	40 mol% NaFSI/C ₃ mpyr[FSI]	76	8C	2000	90	[84]
Rate and temperature	O3-Na _{2/3} Fe _{2/3} Mn _{1/3} O ₂	42 mol% NaFSI/P ₁₁₁₁₄ [FSI]	184	C/10	–	50	[95]
Salt, rate, and temperature	Na _{0.44} MnO ₂	20 mol% NaClO ₄ /C ₄ mpyr[TFSI]	115	C/20	–	75	[74]
Rate and cyclability	Na ₂ FeP ₂ O ₇	56 mol% NaFSI/KFSI	91	–	10	90	[127]
Rate and potential window	Na _{2/3} Fe _{1/3} Mn _{2/3} O ₂	20 mol% NaFSI/C ₃ mpyr[FSI]	227	C/12	20	90	[116]
Rate and temperature	TiO ₂ /C	20 mol% NaFSI/C ₃ mpyr[FSI]	275	–	10	90	[118]
Rate and temperature	HC	10 mol% NaFSI/C ₃ mpyr[FSI]	260	–	50	90	[55]
Current density	Na ⁰	45 mol% NaFSI/P ₁₁₄₁₄₁₄ [FSI]	2.5 ^{a)}	–	0.5 ^{a)}	50	[58]
Rate and temperature	P2-Na _{2/3} Fe _{2/3} Mn _{1/3} O ₂	55 mol% NaFSI/N ₂ (2O2O1) ₃ [FSI]	116	C/10	–	50	[181]

^{a)}Areal measurements, with unit mA cm⁻².

2.2. Conductivity Behavior

Unsurprisingly, for Na IL solutions, the ionic conductivity is highest for low salt concentrations and is usually in the range of 1–10 mS cm⁻¹ near room temperature (20–25 °C). Comparing the conductivity data for imidazolium ionic liquid electrolytes, increasing the cation size from ethyl-methylimidazolium to butyl-methylimidazolium ([C₂mim]⁺ to [C₄mim]⁺, i.e., increasing the alkyl chain length) reduces the conductivity for low salt concentrations from 6.8 to 3.1 mS cm⁻¹ for 2.5 mol% NaTFSI solutions with a similar degree to high 20 mol% concentrations of NaTFSI/C₂mim[TFSI]: 2.8 mS cm⁻¹ and NaTFSI/C₄mim[TFSI]: 1.3 mS cm⁻¹, decreasing by around 55%.^[77] The difference in conductivity is mainly related to the reduction in chain length, this is also reflected in the improvement in conductivity when changing from a methyl to a protic pyrrolidinium ionic liquid for 0.3 M NaTFSI in C₄mpyr[TFSI] (1.3 mS cm⁻¹) versus C₄Hpyr[TFSI], (1.5 mS cm⁻¹).^[86]

Similar to the trend observed for the T_g, [FSI]⁻ has a plasticizing effect and thus these electrolytes show a higher conductivity than their [TFSI]⁻ analogs. For example, 20 mol% NaFSI in C₂mim[TFSI] exhibits a conductivity value of 2.8 mS cm⁻¹ versus 8.5 mS cm⁻¹ in C₂mim[FSI].^[77,79] A similar trend has also been observed for the N₂(20201)₃[TFSI] systems where NaFSI addition showed a higher conductivity than the corresponding NaTFSI salt solutions with 9.9 × 10⁻⁵ S cm⁻¹ versus 1.1 × 10⁻⁵ S cm⁻¹, respectively.^[82,83] While these systems follow the trend expected from their T_g, this is not true when comparing imidazolium and pyrrolidinium analogs. Adding various sodium solutes to C₄mpyr[TFSI] has shown that the highest conductivities were achieved when adding 1 M NaDCA (1.5 mS cm⁻¹)^[77] or NaBF₄ (1.9 mS cm⁻¹)^[74] to the IL while NaPF₆^[77] and NaTFSI^[74] solutions showed the lowest conductivity, each ≈0.5 mS cm⁻¹.

2.3. Sodium-Ion Speciation

Interactions and solvation within the electrolyte, including speciation of the Na⁺ charge carrier as well as aggregation and clustering of the ionic species are all of crucial importance in electrolytes. While it is true that the electrostatic interactions between ions in ILs is weak by definition (i.e., low melting point/lattice energies), the dilute salt solutions commonly used as electrolytes are very different to the situation in ILs which are entirely made of ions and thus interactions, even if weak, are expected to play a significant role.

One way to estimate the degree of interaction is by using the Walden rule which is based on the relationship between conductivity and viscosity. Since these are inversely proportional to one another, the Walden rule states that the product of viscosity η and molar conductivity Λ is constant, shown in Equation (1)^[18]

$$\Lambda \cdot \eta = k \quad (1)$$

Thus viscosity and conductivity data can be converted into a Walden plot shown in Figure 1 where a shift away from the values expected for an ideally dissociated 0.1 M KCl solution indicates a departure from ideality. Typically in an IL this

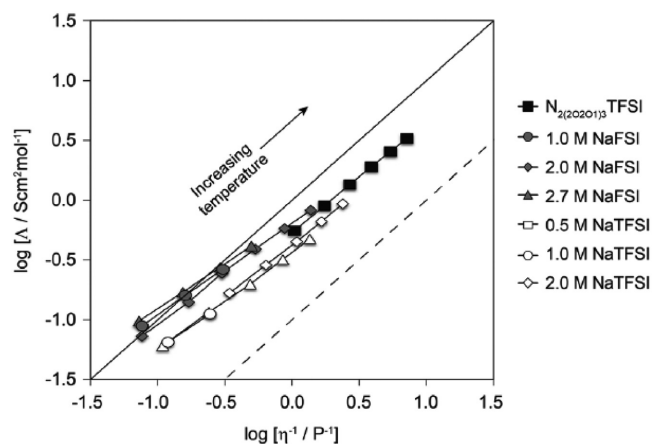


Figure 1. Walden plots describing the departure of measurements from ideality of N₂(20201)₃[TFSI] ionic liquid electrolytes. Reproduced with permission.^[82] Copyright 2017, Royal Society of Chemistry.

is reflected as a reduction in molar conductivity (for a given viscosity) compared to the “ideal line” and is caused by ion association in the IL electrolyte.

While IL electrolytes do not show ideal dissociation, the effects of ion association are usually limited (<10% reduction of the molar conductivity value expected for an ideal solution).^[82,87] This is in agreement with the chemical nature of ionic liquids which suggests low electrostatic interactions between the ions resulting in low melting points. Interestingly, the Walden plot for the NaFSI/KFSI system lies above the ideal KCl line.^[87] This behavior means that the molar conductivity is higher than expected based on the viscosity and suggests decoupling of the viscosity from translational motion. This can be described by the coupling constant, γ , of the fractional Walden rule^[18] described in Equation (2) which has also been applied to ionic liquid electrolytes^[82,87]

$$\Lambda \cdot \eta^\gamma = k \quad (2)$$

Spectroscopic techniques such as nuclear magnetic resonance (NMR),^[64,82,83,88] or vibrational spectroscopy, e.g., IR or Raman,^[64,77] often in combination with computational methods such as molecular dynamics (MD) or density functional theory (DFT) simulations,^[77,88,89] have been applied to study interactions in IL electrolytes. For the C₃mpyr[FSI] system, upon Na⁺ addition a broadening and shift was observed in the signal associated with the ionic liquid's FSI bands caused by interactions involving Na⁺ and [FSI]⁻. The same is true for the Raman bands observed in C₂mim[TFSI] and C₄mim[TFSI] systems which together with DFT calculations suggest the presence of predominantly [Na(TFSI)₃]²⁻.^[88] Similar complexation has been reported for the [FSI]⁻ anion in the NaFSI/C₄mpyr[FSI] system using Raman and AFM techniques.^[90] NMR studies of NaTFSI/N₂(20201)₃[TFSI] and the mixed anion system (NaFSI/N₂(20201)₃[TFSI]) suggest a similar coordination environment for Na⁺ since diffusion in both systems was similar.^[82,83]

A detailed study was performed on the NaFSI/C₃mpyr[FSI] system (NMR studies and MD simulations) which showed that at higher concentrations Na-FSI clusters are formed in which one [FSI]⁻ anion binds two Na⁺ cations.^[88] More recently it has

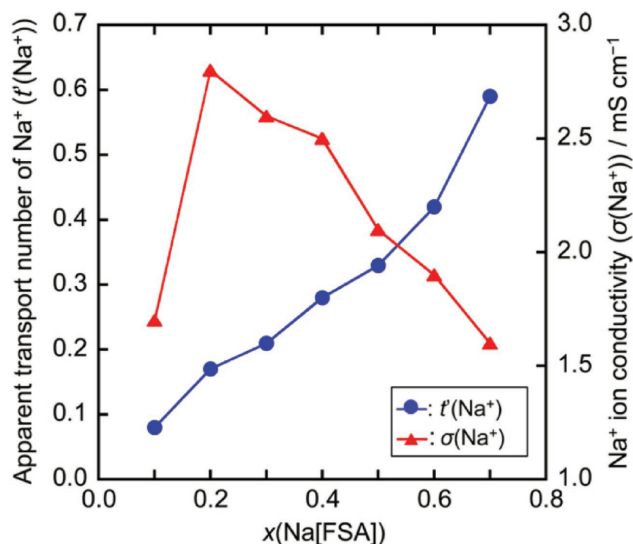


Figure 2. The relationships of Na^+ concentration with ion conductivity (σ) and the apparent transport number (t_{Na^+}) revealing the benefits of superconcentrated electrolytes, i.e., shown here are several mol fractions of NaFSI salt in $\text{C}_3\text{mpyr}[\text{FSI}]$ electrolyte. Reproduced with permission.^[92] Copyright 2015, American Chemical Society.

been shown that with NaFSI concentrations above 50 mol% in this ionic liquid, extensive clustering occurs with a percolating pathway for the Na^+ cation which leads to an effective increase in the diffusion coefficient relative to the other ions in the system.^[91] Such structuring allows for rapid site exchange through structural rearrangement and hence higher diffusion. This could then explain the observations that a higher Na^+ transport number is obtained for higher NaFSI concentration in the ionic liquids (Figure 2).^[49,92] Despite lower ionic conductivities of the electrolyte and the detrimental higher viscosity inherent to ILs, higher concentrations of sodium salt leads to good performance at high Na salt concentrations in Na devices.

2.4. Electrochemical Properties

While the physicochemical properties provide good initial guidelines, the evaluation of key electrochemical properties using techniques such as cyclic voltammetry (CV), Na|Na symmetric cell cycling and calculating sodium transport numbers (t_{Na^+}), is key to predicting device performance. Many systems have been shown via CV to support reversible $\text{Na}^{0/+}$ cycling including ammonium,^[75] pyrrolidinium,^[65,80,81,86,88,93] imidazolium,^[79,94] and phosphonium^[58,95] ionic liquids as well as eutectic salt melts.^[87,96,97] Sodium metal symmetric cell studies provide further evidence of the electrolytes' ability to sustain sodium electrochemistry over long periods. In these experiments, sustained low overpotentials reflect effective Na^+ ion transport and good electrochemical stability. Very low overpotentials of 10–90 mV were observed when plating and stripping Na^0 for NaFSI in trimethyl-isobutylphosphonium bis(fluorosulfonyl)imide ($\text{P}_{11114}[\text{FSI}]$) when galvanostatically cycled at 0.025–1.0 mA cm^{-2} ,^[95] and similarly with the related methyl-triisobutylphosphonium analog ($\text{P}_{114i4i4}[\text{FSI}]$) when using a variety of salts such

as NaFSI/NaTFSI: 30–110 mV or NaPF_6 : 70–180 mV at current densities of 0.1 mA cm^{-2} or 0.25 mA cm^{-2} .^[98] In the latter system, Makhlooghiazad et al. reported that the overpotentials were also dependent on the choice of separator and ranged from 55 to 100 mV when cycled at 0.25 mA cm^{-2} .^[58] These are all examples of high salt content systems exhibiting remarkably low overpotentials and compatibility at a Na^0 electrode. Sodium dicyanamide in *N*-butyl-*N*-methylpyrrolidinium dicyanamide ($\text{NaDCA}/\text{C}_4\text{mpyrDCA}$) has also been cycled with similarly low potentials of 100 mV at a Na^0 electrode, although at low current densities of 0.01 mA cm^{-2} .^[65] The lowest reported overpotentials, 10–50 mV, were obtained for ammonium electrolyte solutions ($\text{NaFSI}/\text{N}_{1116}[\text{FSI}]$, $\text{NaFSI}/\text{N}_{1144}[\text{FSI}]$, $\text{NaFSI}/\text{ASN}_{(4,4)}[\text{FSI}]$) at impressive current densities of 1.0 mA cm^{-2} when using glass fiber separators.^[75]

2.5. Na-Ion Hybrid Electrolytes

It has become increasingly recognized that the mass transport properties of ionic liquids can be further improved through mixing with molecular solvents as these molecular solvents exhibit higher conductivities at moderate temperatures.^[99] Such ionic liquid–molecular solvent systems have been called “hybrid-electrolytes” in the sense that they combine the properties of both solvent systems, sometimes in a synergistic fashion. A variety of solvents have been investigated, some of which represent simple “diluent,” for example, toluene, and others which are well known aprotic electrolyte solvents in their own right, for example, acetonitrile and propylene carbonate.^[100] The majority of the solvents used in reports are aprotic solvents, this most likely originates from the perceived instabilities of the protic solvents in sodium metal based cells. However as we highlight in Section 2.6 a protic solvent such as water has shown some stability indicating that protic solvents may also be a possible avenue of hybrid research. In the case of battery electrolytes the solvent systems used are those traditionally well-understood in the area, including the organic carbonate mixtures. One of the advantages of such mixtures is that the overall cost of the ionic liquid based electrolyte is lowered.

While the transport properties tend to improve smoothly with molecular solvent content, the effect of Henry's Law tends to maintain a low vapor pressure of the volatile solvent such that the attractive thermal properties of the ionic liquid are not immediately diminished. For example, Figure 3 compares the flammability of a pure carbonate organic electrolyte and a 50:50 mixture of ionic liquid and carbonate electrolyte; the very low flammability of the ionic liquid is maintained in the hybrid electrolyte despite the presence of the organic component. For this reason, hybrid electrolytes are being reported for Li and Na battery applications. Plylahan et al. have recently investigated hybrid C_3mpyr atomic force microscopy [TFSI]–carbonate mixtures for use in high temperature lithium-ion batteries based on LiFePO_4 demonstrating stable cycling at 80 °C.^[17] Egashira et al. show a hybrid propylene carbonate (PC)/ $\text{N}_{122(201)}[\text{TFSI}]$ tends to inhibit insertion of sodium into hard carbon electrodes, particularly at higher fractions of IL near 70 vol%.^[101] Monti et al. have shown that in hybrid mixtures of 0.8 M $\text{C}_4\text{mim}[\text{TFSI}]$ or $\text{C}_3\text{mpyr}[\text{TFSI}]$ with ethylene carbonate and propylene carbonate

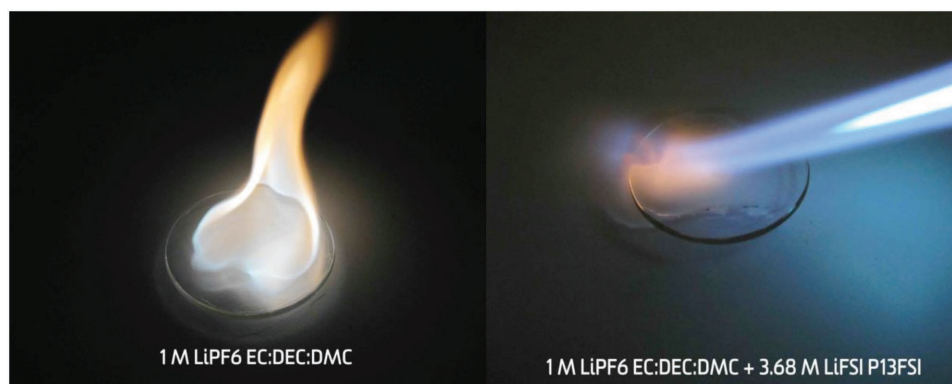


Figure 3. Pure organic electrolyte (left) and a hybrid 50% organic electrolyte-ionic liquid exposed to a naked flame.

that the electrolytes are less ignitable/more stable than uncoordinated solvent.^[102] It is interesting to note that the organic solvents do remain after ignition to a certain degree, and, that these remnant organic solvents do so because they are strongly coordinated by Na^+ . This is revealed by comparison of FTIR spectra before and after burning.

Transport and thermodynamic properties can show a variety of effects beyond what can be thought of as “simple-mixing” rules and these are in many cases advantageous to device performance. **Figure 4** provides an illustration of the effect of an organic electrolyte (ethylene carbonate/propylene carbonate (1:1 by volume) in mixtures of ionic liquid $\text{C}_3\text{mpyr}[\text{TFSI}]$, with 1 M NaFSI as the sodium salt.^[103] It is notable that the 25% by volume mixture has conductivity which is similar to that of the standard organic electrolyte. In another study, Monti et al. have also shown good cycling performance of hard carbon (HC) Na-ion anodes in an electrolyte comprised of 0.8 M NaTFSI in a mixture of 90 wt% (EC:PC 1:1) and 10 wt% $\text{C}_3\text{mpyr}[\text{TFSI}]$ demonstrating 182 mAh at C/10 over 40 cycles.^[102] By moving to a ternary electrolyte containing PEGDME, a sodium salt and ionic liquid N,N -diethyl- N -methyl(2-methoxyethyl)ammonium, $\text{N}_{122}(\text{201})$, Egashira et al. formulated a hybrid electrolyte with a ratio of 8:1:2 that reaches a high conductivity of 1.2 mS cm^{-1} at room temperature.^[72]

Interestingly, the benefits of employing such mixtures reach considerably beyond cost and improved mass transport proper-

ties. Synergistic effects in the formation of the SEI layer on Li cathode materials were described by Theivaprakasam et al.^[104] Similar effects are currently being explored in Na electrolytes by Manohar et al.^[103] For example, **Figure 5** shows the cycle performance of a Na vanadium phosphate $\text{Na}_3\text{V}_2(\text{PO}_4)_3$ cathode material in various hybrid electrolyte mixtures of $\text{C}_3\text{mpyr}[\text{TFSI}]$ and an organic electrolyte EC/PC (1:1 by volume) with 1 M NaFSI as the sodium salt. The 50% by volume hybrid shows distinctly superior cycling performance. Electron microscopy and X-ray photoelectron spectroscopy were used to study the SEI layers on cathodes that had been subjected to 100 cycles at C/2 and it appears that the hybrid electrolyte produces a less resistive, more highly Na^+ ion-permeable SEI layer compared to the organic electrolyte. The result is more stable cycling performance with no sign of significant capacity loss over the cycles so far studied.

2.6. Presence of Water

For some time now the scientific community has been aware of the drawbacks that adventitious moisture can apply within ionic liquids;^[22] water severely truncates the electrochemical window of neat electrolytes and thus limits the potential range of applications.^[105–107] A report by Randström et al. clearly demonstrated a simple cyclic voltammogram to measure

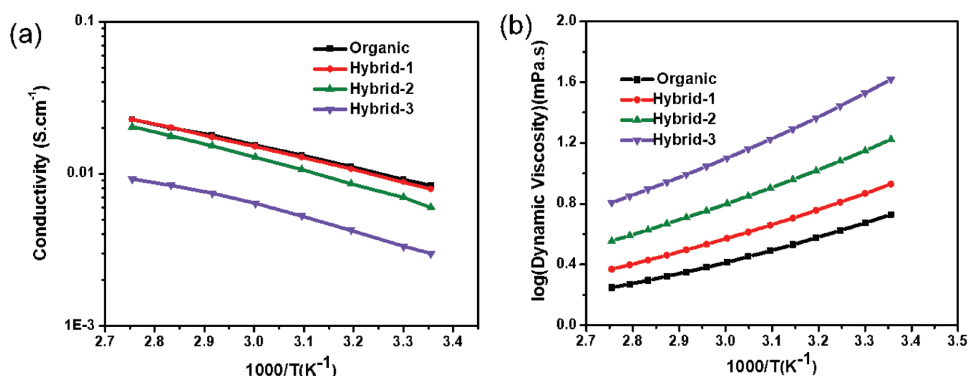


Figure 4. Conductivity and viscosity of EC:PC- $\text{C}_3\text{mpyr}[\text{TFSI}]$ hybrid electrolytes showing the progressive enhancement of transport properties as the molecular solvent content increases. Hybrids 1, 2, and 3 are 25, 50, or 75% v/v $\text{C}_3\text{mpyr}[\text{TFSI}]$ mixtures with organic solvent (EC:PC 1:1), 1 M NaFSI added in all cases. Reproduced with permission.^[103] Copyright 2018, Royal Society of Chemistry.

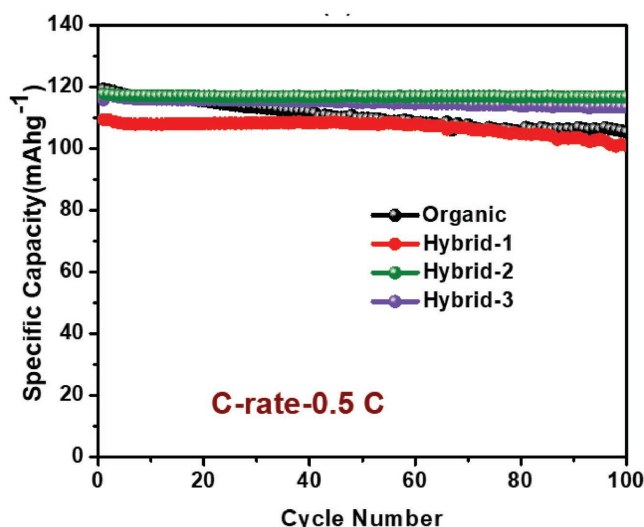


Figure 5. Cycle performance of a Na|hybrid electrolyte|NVP device with organic and IL hybrid electrolytes at 0.5C. Hybrids 1, 2, and 3 are 25, 50, or 75% v/v $C_3\text{mpyr}[\text{TFSI}]$ mixtures with organic solvent (EC:PC 1:1), 1 M NaFSI added in all cases. Reproduced with permission.^[103] Copyright 2018, Royal Society of Chemistry.

the devastating influence of as little as 800 ppm of water on the cathodic stability of $C_4\text{mpyr}[\text{TFSI}]$.^[107] It has since been a requirement of studies carried out in the field of ionic liquid research to include moisture contents, typically measured via Karl Fischer titration or electrochemical methods, usually limited to <100 ppm.^[108] The inclusion of excess water within an ionic liquid electrolyte has been highly avoided, or strictly controlled, responsible for altering the mechanism of metal electrodeposition^[109] and by their very nature incompatible with Li metal when included in electrolyte formulations.^[26]

However water can be used as an additive diluent to ionic liquid electrolytes that oftentimes exhibit lower conductivity and increased viscosity than organic solvents. **Figure 6** shows the conductivity of neat $C_3\text{mpyr}[\text{FSI}]$ ($\text{H}_2\text{O} > 20$ ppm) and three electrolyte solutions including NaFSI salt that also contain differing amounts of water addition, i.e., the neat $C_3\text{mpyr}[\text{FSI}]$ and <20 ppm H_2O electrolyte systems are both considered dry. Figure 1a shows us how the decreased conductivity upon increased

salt content of 50 mol% NaFSI within $C_3\text{mpyr}[\text{FSI}]$ can be alleviated by incremental water addition up to 500 ppm,^[110] with the 500 ppm 50 mol% electrolyte approaching conductivity values of the neat and dried $C_3\text{mpyr}[\text{FSI}]$. This increase in conductivity is of course shared by the decrease in viscosity, however note well the clear gap still remaining between the neat IL and the “wet” electrolytes shown in Figure 6b. Unlike the reported disadvantage >100 ppm water has had on Li^0 and Na^0 cycling performance when using a $[\text{DCA}]^-$ anion,^[26,65] the addition of 500 ppm of water to this $[\text{FSI}]^-$ based electrolyte was shown to have a negligible effect on Na|Na symmetrical cell cycling. For example, Basile et al. describe that the addition of water beneficially influences the prepared surfaces when cycling using these water containing 50 mol% NaFSI/ $C_3\text{mpyr}[\text{FSI}]$ electrolytes. However, further study into the effect of water additives within ionic liquid electrolytes is necessary for the benefit of cell performance and also production, particularly with the wide variety of cations and anions available. These observations also suggest that alternative protic solvents may also be effective additives in sodium based cells.

3. Sodium Cells Employing Ionic Liquids

Currently, the higher costs of low volume batch synthesis for ionic liquids is somewhat prohibitive for their implementation as electrolytes within energy storage. The cost of these ILs is predominantly due to the anion chemistry in use, whereas the organic cations are relatively inexpensive. This cost is expected to decrease through economy of scale, however it is difficult to estimate the commodity price of an ionic liquid electrolyte formulated for sodium cells. Using BatPaC 3.1 (lithium battery simulator) as an analog for a similar sodium based technology, the projections of cost for production of an integrated battery pack can be estimated.^[111] Assuming that the cost of an IL electrolyte is double that of conventional electrolyte (est. \$17 L^{-1}) currently used in Li-ion technologies, the estimated battery pack total increases by 10% across a range of 7 different cell chemistries. To go further, tripling the electrolyte cost increases the battery pack total 15–20% dependent on the materials chemistry of the battery. Hence, if sodium based batteries incorporating ionic liquids can provide sufficient performance

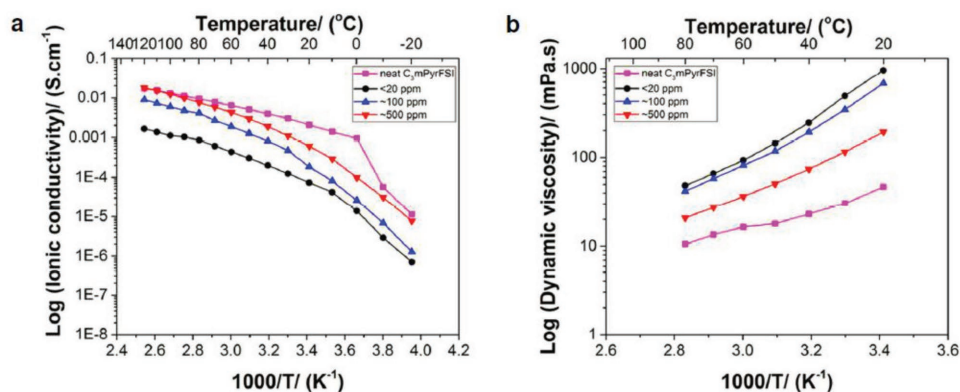


Figure 6. Conductivity and associated viscosity of the pyrrolidinium ionic liquid electrolyte with water as an additive to superconcentrated NaFSI/ $C_3\text{mpyr}[\text{FSI}]$. Reproduced with permission.^[110] Copyright 2017, Elsevier.

advantages, these batteries will be cost competitive with conventional cells. This highlights the fact that the electrolyte itself is not a large contributor to battery pack cost, rather the minerals required to prepare cathode materials such as Co and Mn are. This arises due to the large capital and CO₂ emissions required when mining these commodities. It should also be noted that beneficial cell performance has been reported when these ionic liquids are superconcentrated. Through addition of salt to the IL the cost can be dramatically decreased. This is especially relevant with continued efforts to develop new low cost processes to prepare LiTFSI salts at comparable price to LiPF₆.

With the physicochemical properties of ionic liquids established, and the resultant electrochemical properties promoting these electrolytes for sodium battery applications, many formulations have been paired with anode and cathode materials to investigate sodium battery device performance.^[59,74,84,86,87,93–96,112] The ionic liquid electrolytes most investigated are those including the pyrrolidinium cation, NaFSI/C₃mpyr[FSI]^[56,84,113–118] and NaTFSI/C₄mpyr[TFSI].^[59,86,93,112,113,119–121] due to their popularity in lithium technologies.^[27,30] It should also be noted that whilst the physicochemical properties of tertiary or polymer based electrolytes have not been discussed in depth thus far, a number of battery prototyping experiments have been reported.^[63,64,68,70,71]

3.1. Sodium Cell Chemistries

While a wide range of sodium/ionic liquid electrolyte prototype devices have been prepared and studied recently, including Na–O₂,^[119] Na–S,^[68] dual-ion Li/Na cells,^[122] poly(3,4-ethylenedioxythiophene) polystyrene sulfonate (PEDOT)/lignin hybrid cells,^[121] as well as a catholyte battery^[94] the focus of this section is on Na-ion and Na-metal cell research employing ionic liquid electrolytes. Listed in **Table 3** are studies of ionic liquid performance versus a variety of electrodes, highlighting the composition of the ionic liquid electrolyte and the chemistry of the electrode. As performance indicators, we have included discharge capacities and rate capability together with the cycling temperature for several reports. For comparison amongst these studies, the convenient form of C-rate has been calculated for those studies who report only current density. These are converted using the theoretical capacity assuming 100% reversible sodiation/desodiation. Various cathode and anode materials have been employed in the ionic liquid electrolyte field. Cathodes typically belong to the class of layered transition metal oxides or polyanionic materials, while the anodes are either hard carbons, titania based, or metal alloys.^[123]

Transition metal oxide electrodes have been predominantly studied to date, with the NaCrO₂ found in several reports from the Hagiwara group.^[84,87,93,114,124,125] The structure of transition metal oxides is described as either octahedral or prismatic together with a number which describes the stacking order of the layers.^[126] Polyanionic cathodes that are listed herein are based on phosphates, NaFePO₄,^[59,112,117] Na₂FeP₂O₇,^[127] NaVOPO₄,^[128] and Na₃V₂(PO₄)₃,^[86,129] and the silicate Na₂MnSiO₄.^[115] Regarding studies at the negative electrode, anodes composed of carbon materials^[55,56,113,124,130] are most prevalent in the literature, owing to the vast amount of knowledge around carbon intercalation negative electrode materials from studies cov-

ering decades toward alkali rocking-chair batteries. There are also several reports on the efficient performance of TiO₂ based anodes^[131,132] and other alloying materials.^[133] As the majority of studies carried out thus far have used a sodium metal counter electrode, i.e., within symmetrical and half-cell geometries, the majority of the electrolytes employed have been proven compatible with Na metal electrodes.

The use of ionic liquids as electrolytes has a clear advantage over the conventional organic carbonates given the intrinsic high boiling points highlighted previously. This is obvious when reviewing the literature as many of the studies included in **Table 3** are conducted at intermediate and elevated temperatures. This also assists researchers in alleviating the large viscosity and mass transport limitations. However, the melting point of sodium at 97 °C itself must also be factored in when conducting these experiments. By increasing the temperature the capacity of an electrode material is increased. Additionally, it should be expected that the increased temperatures will impact favorably upon the kinetics of redox reactions taking place.

Higher operating temperatures are reported for cells comprising pyrrolidinium electrolytes cycled with layered transition metal oxides; NaCrO₂,^[84,93,114,124] Na₂MnSiO₄,^[115] Na_{0.44}MnO₂,^[74] NaFePO₄,^[59,112,117] as well as HC anodes.^[113,124] While most studies focus on the temperature range 20–90 °C, Ding et al. reported an investigation of the cycling performance of Na|NaFSI/C₃mpyr[FSI]|NaCrO₂ cells over a wide temperature range of –20 to 90 °C.^[84,114] They showed there was a dramatic increase in the capacity when the temperature was increased to 25 °C regardless of the Na⁺ concentration. Beyond that temperature the cycling performance did not improve significantly. It was determined that below 0 °C, a 25 mol% NaFSI/C₃mpyr[FSI] electrolyte is the optimum concentration in these cells (**Figure 7**). At increased temperatures of 90 °C, a concentration of 40 mol% performed best. This alludes to the existence of an optimum range of Na⁺ ion concentration depending upon the operating temperature of the given application. While the capacity of the Na|NaFSI/C₃mpyr[FSI]|NaCrO₂ system is lower at low temperatures (0 °C), the stability is better than devices cycled at 90 °C. For full cells when using hard carbon (HC|NaTFSI/C₃mpyr[TFSI]|NaCrO₂) it was reported that there is no temperature dependence of the stability.^[114] When comparing the impedance of the HC and Na⁰ electrodes at low temperatures, the reports suggest that the impedance of the HC electrode was of similar magnitude and slightly lower compared to the corresponding Na electrode (0–90 °C).^[113] Even though the C₃mpyr[FSI] ionic liquid has shown promising compatibility with hard carbon electrodes, the inclusion of K⁺ inclusive ILs, e.g., KFSI doped NaFSI/C₃mpyr[FSI] or simply NaFSI/KFSI, is not suitable due to the irreversible K⁺ ion insertion into hard carbon.^[55]

With increasing salt content the mobility of electrolytes drop due to an increase in intermolecular interactions. Thus it would be expected that device performance is best at low salt concentrations, e.g., where the viscosity is low and the conductivity is high. However, as discussed in the previous section, the electrochemical properties of high salt content systems can often outperform the low. In fact, it has been observed that with increasing salt content the cycling performance is indeed promoted. For the Na|NaTFSI/C₄mpyr[TFSI]|NaFePO₄ cell described by Wongthitharom et al. the capacity retention

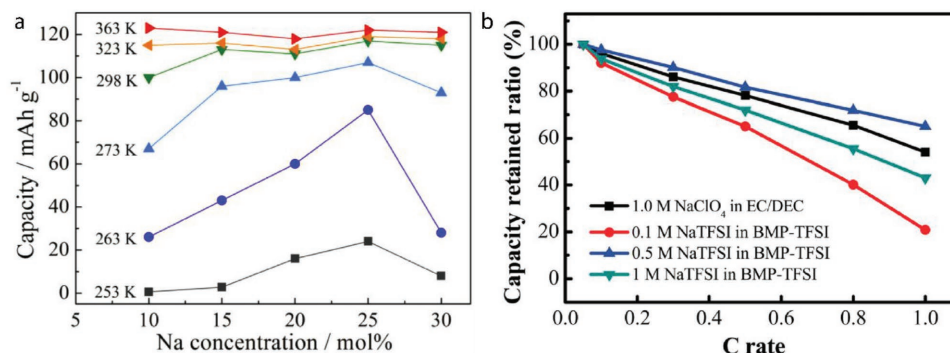


Figure 7. Capacity measurements. a) The temperature dependence of concentrated ionic liquid electrolytes for NaCrO₂ capacity retention in Na[NaFSI]/C₃mpyr[FSI]/NaCrO₂ cells at concentration between 10–30 mol% and b) the capacity retention as a function of salt concentration and C rate in Na[NaTFSI]/C₄mpyr[TFSI]/NaFePO₄ cells. (a) Reproduced with permission.^[84] Copyright 2014, Elsevier. (b) Reproduced with permission.^[112] Copyright 2014, Royal Society of Chemistry.

increases with greater concentration from 0.1 to 0.5 M (Figure 7b).^[112] Although in that case, beyond 1.0 M the capacity drops off across the breadth of C-rates tested. This has also been observed for NaBF₄/C₄mpyr[TFSI] electrolytes.^[59] At this moderately low concentration, the initial improvement in performance may simply be a result of the increased number of charge carriers which allow for more efficient intercalation/extraction of Na⁺, while the drop at moderate concentrations (around 1 M) may be attributed to the poorer transport properties observed at higher concentrations; this is somewhat in contrast to the superconcentrated [FSI]⁻ systems discussed earlier.

Additionally, it has been observed that the ionic liquids indeed can outperform conventional solvent based electrolytes in terms of capacity, stability, high temperature performance, and safety. The 1 M NaBF₄/C₄mpyr[TFSI] electrolytes show better cycling performance as compared to solutions with NaTFSI or NaPF₆ and their conventional organic carbonate equivalent, shown in Figure 8.^[59] This is also true for the Na[Na_{2/3}Fe_{2/3}Mn_{1/3}O₂ (P2/O3) cells Hilder et al. has reported with a variety of ionic liquid electrolytes^[95] and the abovementioned Na[NaTFSI]/C₄mpyr[TFSI]/NaFePO₄ cell.^[112] Importantly, the sodium salt added to those ionic liquids has an effect on the cycling performance as well.

Although there have only been limited reports on full cells, promising performances have been published in coin-cell

geometries.^[86,113] The recent report of the operation of the electrochemically inactive Maricite phase NaFePO₄ cathode at 90 °C in a pyrrolidinium FSI ionic liquid, with good stability and 100 mAh g⁻¹ specific capacity after 120 cycles, opens a new avenue of research by broadening the scope of useful cathode materials for moderate temperature (nominally 60–150 °C) battery applications.^[117] Additionally, in the short time span of sodium ionic liquid electrolyte research, Fukunaga et al. have described a prototype 27 Ah prismatic cell based on HC[NaFSI]/C₃mpyr[FSI]/NaCrO₂ which delivered energy density and specific energy of 125 Wh L⁻¹ and 75 Wh kg⁻¹ respectively.^[124] The full cell displays energy efficiency of 96.8% at 50 °C comparable with coin cell variants. At long cyclability scales, the prismatic cell exhibited 90% capacity retention after 1000 cycles. This development builds upon the growing number of studies investigating the compatibility of hard carbon materials with ionic liquids, predominantly pyrrolidinium FSI.^[55,56,113,134]

Another full cell arrangement includes an alloying anode using a nanostructure Sb–C composite material which has also shown promise versus P2-Na₂NiFeMnO₂ layered oxide cathode in a NaTFSI/C₄mpyr[TFSI] electrolyte.^[135] These preliminary results of this cell show compatibility of the ionic liquid electrolyte at low salt concentration (0.2 M) with both electrodes exhibiting 100 mAh g⁻¹ and 2.7 V working voltage.

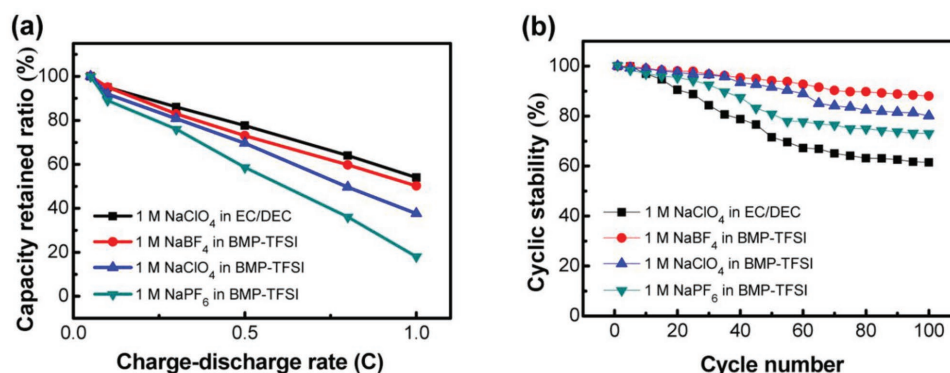


Figure 8. a) Salt dependence upon charge–discharge rate in C₄mpyr[TFSI] ionic liquid electrolytes within Na[NaFePO₄] cells, and b) the cyclic stability of these cells surpassing conventional electrolytes at 0.3C rate and 50 °C. Reproduced with permission.^[59] Copyright 2014, American Chemical Society.

3.2. Metal–Air

Metal–air batteries are a promising candidate for the next generation of energy storage devices owing to their intrinsically high energy-density values.^[136] Among all the battery chemistries, Na–O₂ has emerged as an interesting alternative to conventional Li-ion due to their high specific energy (i.e., 1605 or 1108 Wh kg^{−1}, depending on the final discharge product),^[136] their low production costs and the global abundance of sodium.^[137] The parameters to control the formation of a specific discharge product in Na–O₂ are still unclear. However, development of electrolytes has been a route of extensive and widespread interest to improve the performance of the metal–air battery technologies in general. In that regard, ionic liquids, due to the large variations in anion–cation composition, allow one to optimize the electrolyte properties and performance.

One of the first demonstrations of ionic liquids as electrolytes for Na-air batteries was reported by Zhao et al.^[138] In that work, *N*-methyl-*N*-propylpiperidinium bis(trifluoromethanesulfonyl) imide (C₃mpip[TFSI]) was evaluated as a potential electrolyte and the performance was comparable with carbonate and ether-based electrolytes. Discharge products were composed of parasitic products (carbonates and hydroxides) and NaO₂ for every cell configuration, however the ratio of each component was strongly dependent upon the nature of the electrolyte. Therefore, in order to clearly understand and control the discharge products and avoid the generation of parasitic products, it is necessary to gain insight into the nucleation processes occurring from the bulk electrolyte at the electrode/electrolyte interface. However, currently there is a dearth of extensive information on the reduction mechanism corresponding to Na–O₂ in ionic liquids and the impact on the discharge products.

Recently, there has been a focus on gaining a fundamental understanding of the species generated in the bulk ionic liquid electrolyte in the presence of the electrogenerated superoxide anion, O₂^{•−}. This has been investigated by Pozo-Gonzalo et al. using a conventional 3-electrode set-up.^[119] In that study, the concentration of the salt greatly affected the stabilization of superoxide. Through the use of experimental and theoretical calculations,^[119,139] it was revealed that when at higher [Na⁺] (0.7 mol% to highly saturated 16.6 mol%) the superoxide coordination environment shifts away from [C₄mpyr]⁺ toward the Na⁺ cation itself and impacts the oxygen reduction reaction mechanism in the C₄mpyr[TFSI] electrolyte.

Of all the ionic liquids studied more broadly in relation to the ORR reaction, aliphatic and alicyclic ammonium-based ILs are known to stabilize the superoxide anion. Thereby making them good candidates as electrolytes for metal–air batteries.^[140] The mechanism of the ORR in neat C₄mpyr[TFSI] has been studied in detail and the process assigned to the one-electron reversible O₂/O₂^{•−} redox couple.^[141]

The generation of a complex species, [O₂^{•−}][C₄mpyr⁺]_{*n*}[Na⁺]_{*m*}, is envisioned in the bulk sodium cation pyrrolidinium-based ionic liquid with the composition depending on the Na⁺ concentration. Additionally, Pozo-Gonzalo et al. established that the coordination between Na⁺ and [TFSI][−] governs the mobility of the superoxide anion as determined by the simulated diffusivities shown here for the first time in **Figure 9**. The interesting trend of the diffusion coefficient of superoxide can be explained

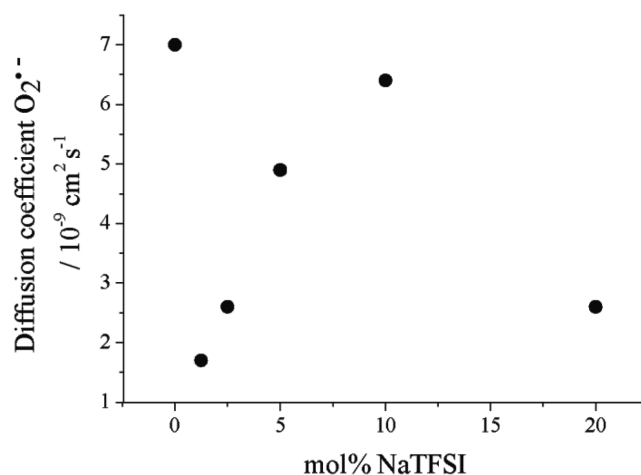


Figure 9. Calculated diffusivities for the superoxide anion in neat C₄mpyr[TFSI] and NaTFSI/C₄mpyr[TFSI] electrolyte mixtures.

by the combination of different factors. The sharp decrease in the diffusion coefficient in the presence of 2.5 mol% Na⁺ can be explained as the result of the stronger interaction between the superoxide anion and Na⁺, which slows down the diffusion of superoxide D(O₂^{•−}).

Upon increasing the NaTFSI concentration, the number of [C₄mpyr]⁺ cations coordinated to superoxide will decrease from 4 to 2, thereby leading to a less bulky aggregate and therefore more mobile species. At the same time, there is a competition between TFSI and superoxide anions to coordinate Na⁺. A trend in the coordination has been reported for small alkali cations with sulfonylimide-based anions.^[88,142]

These previous findings are extremely important from an applied perspective to understand the growth mechanism of the discharge products and their morphology.^[143] Using an in-house designed three electrode pipette cell the discharge products on an air cathode has been reported. The work shows that increasing the concentration of NaTFSI salt, from 1.13 to 16.6 mol%, in the C₄mpyr[TFSI] provides a significant enhancement in the discharge capacity by an order of magnitude, in addition to reducing the overpotential and increasing the long-term cyclability. The authors showed that film-like deposits obtained in dilute IL electrolytes produce a more capacitive behavior, whereas a dense coverage of spherical particles, ranging from nanometers to microns in diameter, are observed for highly concentrated mixtures.^[143]

These findings provide evidence that the porous cathode after discharge in the 4 mol% NaTFSI electrolyte mixture is more blocked in comparison with that in the 16.6 mol% NaTFSI electrolyte mixture which prevents oxygen access at the gas–electrode–electrolyte three-phase boundaries. By comparison, the 16.6 mol% NaTFSI electrolyte mixture results in limited passivation and blockage of the electrode surface. Different discharge products were obtained by different nucleation mechanisms and this was suggested to be dependent on the ion speciation in the ionic liquid. Thus there is scope to control the performance of the Na–O₂ cell by controlling the electrolyte properties to further improve battery performance.

3.3. Electrode–Electrolyte Interface

The shortcoming of batteries comprising an alkali metal anode is the anode's susceptibility to failure as a result of unfavorable metal deposits which can form a rough morphology with lower density and dendritic form.^[31] Likewise, cell failure can arise due to an ineffective passivation film which normally arrests continued electrolyte breakdown (i.e., if an ineffective SEI is formed).^[144] The SEI allows the ingress/egress of Na⁺ ions whilst blocking fresh Na⁰ metal which spontaneously reduces the electrolyte. Inhomogeneity of the SEI across an electrode, whether morphology, impedance, or thickness, can play a role in the failure of a sodium cell. Unlike Li⁰ anodes, where dendrites are considered the dominant mode of failure through short circuits, it is the breakdown of electrolyte at the sodium metal surface which is regarded as significantly detrimental.^[145]

There has been much interest in the characterization of the SEI which forms upon the alkali anode since the first^[15] report of an ionic liquid enabling plating/stripping of Li metal.^[27,28,30,146] More recently there have been reports of studies toward understanding the SEI and interfacial structure within sodium based electrolytes,^[48,147] but very few in depth studies with ionic liquid electrolytes.^[58,65,90] A sodium electrolyte based on superconcentrated 5 M NaFSI/DME, which forms a solvate and operates similarly to a superconcentrated ionic liquid, has been used for Na metal cycling with very high Coulombic efficiency of 99.3%.^[48] In that work Lee et al. demonstrated that the higher concentration electrolyte outperforms both 1 M NaFSI/DME and the organic carbonate equivalent (1 M NaPF₆/EC:PC). Using scanning electron microscopy (SEM) and energy dispersive X-ray spectroscopy the study revealed that higher concentrations of salt minimize electrolyte breakdown at the surface of Na metal and promote better SEI formation without tarnishing the anode surface. Due to the number of studies reported, the breakdown of the [FSI][−] anion is well understood through a variety of different approaches in Li systems.^[28,148–150] Another in depth analysis of the SEI by Qian et al. also in a superconcentrated electrolyte, albeit for LiFSI solvated in DME, show how these electrolytes outperform less concentrated analogues and prepare a highly conductive SEI layer.^[47]

Reports generally assume a similar role and performance for an SEI in Na⁰ systems, though limited evidence or detailed analysis is available to date. In actuality, the existing work on defining the character and nature of the SEI on sodium anodes is limited to characterization from X-ray diffraction,^[151] SEM,^[58,86,120,151] and electrochemical impedance spectroscopy (EIS)^[58,59,74,95] – all invaluable tools in the study of surface films such as the SEI. However, of these studies, the investigation of the anode surface is less concerned with the SEI itself, rather, these techniques are used to establish the effect of cycling upon the nature/morphology of the electrode material. The most detailed EIS study to date by Basile et al. provides insight into the evolution of the electrode–electrolyte interface before, during and after cycling from superconcentrated 45 mol% NaFSI/P_{14i4i4}[FSI] in Na|Na symmetrical cells. The equivalent circuit model is not provided, however clear trends of resistance decreases proportional to polarization current densities is demonstrated. Through this observation, enhanced Na|Na metal

symmetrical cell cycling stability was made possible by applying an initial high current rate which prepares an ideal interface for further cycling. Highlighting the compatibility of these electrolytes to Na⁰. There is however a detailed spectroscopic study of the SEI on surface modified Ge for Na-ion electrodes. Lahiri et al. modify a Ge electrodeposit using Sb through an electrodeless deposition in an ionic liquid medium. The formation of a Ge_xSb_{1−x} film identified via Raman and XPS leads to better diffusion of Na⁺ leading toward greater capacity and current densities during half-cell cycling in a NaFSI/C₃mpyr[FSI] electrolyte.^[152] There are no such thorough investigations on hard carbon electrodes at the time of writing however. There is no doubt that understanding the fundamental nature of this interfacial layer can have beneficial impact on the practical cycling of sodium cells.

4. Solid State Na Electrolytes

4.1. Organic Ionic Plastic Crystals

Organic ionic plastic crystal ion conductors are novel solid electrolytes that offer opportunities to improve the safety and performance of Na batteries. OIPCs consist of an organic cation–anion pair, much like those within an IL, however, they have regular crystal structures in the solid state.^[153] Interestingly at temperatures below the melting point (T_m), an OIPC rearranges to a lower symmetry crystalline phase through the rotational motion of ions within the long-range ordered lattice. The presence of these rotator phases leads to one or several transitions from orientationally ordered phases to orientationally disordered ones resulting in an increase in entropy with increasing temperature. Thus, eventually these crystals melt with a remarkably low entropy of fusion ($<20 \text{ J K}^{-1} \text{ mol}^{-1}$).^[153] A consequence of this structural disorder is the formation of defects (vacancies or extended defects such as dislocations) which enables the motion of ions and hence results in ionic conductivity.^[154] These defects also lead to more readily deformable materials, hence the term plastic crystal.

An OIPC may also have many properties in common with ionic liquids including low T_m , low flammability, negligible volatility, good thermal and electrochemical stability and high Li⁺/Na⁺ transference number. Along with the advantageous properties of ILs, OIPCs being solid state materials, have desirable mechanical properties. When comparing OIPCs to molecular plastic crystals, such as succinonitrile,^[155,156] OIPCs are much safer, as succinonitrile is volatile above the melting point—this is closely analogous to the safety benefits of ILs over organic solvents.^[156,157] These properties have made them favorable materials for application as solid electrolytes for improving the safety and reliability of electrochemical devices. Hence they have been proposed as solid state electrolytes in a variety of applications encompassing but not limited to fuel cells,^[24,44] batteries,^[24,157,158] supercapacitors,^[159] and dye-sensitized solar cells.^[160,161]

Thus far, only a few studies have been conducted on OIPC solid electrolytes for Na battery applications^[162–165] in contrast to the more numerous reports of OIPCs as solid-state electrolytes for Li cells.^[54,166–172] Adding a second salt component to

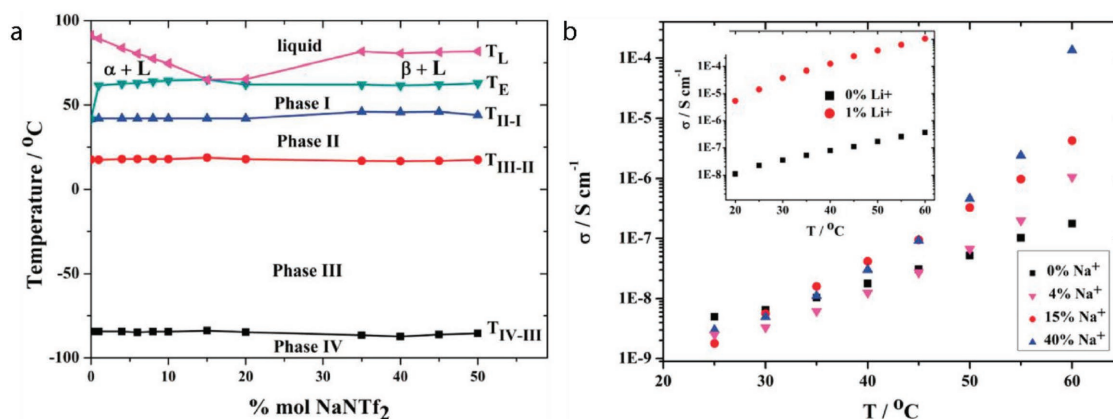


Figure 10. a) Phase diagram of NaTFSI/C₂mpyr[TFSI]. The phases are labelled I through IV with the highest temperature phase always being labeled as Phase I, and b) Ionic conductivity of pure C₂mpyr[TFSI] and mixed NaTFSI/C₂mpyr[TFSI]. Reproduced with permission.^[162] Copyright 2014, Royal Society of Chemistry.

OIPCs as target ions (Li⁺ or Na⁺ ions for Li or Na batteries) which is a first step for their application as an electrolyte in devices, usually improves their ionic conductivity.^[166,167,173–176] One hypothesis regarding the mechanism of conduction of Li ions in OIPCs is that orientational and/or rotational motions within the OIPC may benefit the motion of interstitial Li ions.^[177] In addition, the inclusion of additional defects (e.g., vacancies) or decreasing grain size (i.e., increasing the volume of grain boundaries) by adding salts could be responsible for fast conduction of ions in an OIPC.^[157] Alternatively, the formation of a low melting point mixture of an OIPC and Li or Na salts (e.g., eutectics) can lead to higher ionic conductivity. At some temperatures, these mixtures convert to a two-phase liquid/solid material with the liquid component localized at the grain boundaries of the OIPC rich phase, providing pathways for diffusion of ions.^[162–165,176,178]

The phase behavior of a mixture of an OIPC and sodium salt was reported for the first time by Forsyth et al., who examined *N*-ethyl-*N*-methylpyrrolidinium bis(trifluoromethanesulfonyl) imide (C₂mpyr[TFSI]) when doped with up to 50 mol% NaTFSI. The phase diagram was extracted from dynamic scanning calorimetry traces (DSC, **Figure 10**). They reported that this binary system has a eutectic transition at 63 °C at the composition of 15 mol% NaTFSI. Interestingly however, this is different from the eutectic transition temperature and eutectic composition of the same OIPC doped with LiTFSI, previously studied by Henderson et al.^[178] Below the eutectic temperature, two solid phases, one rich in OIPC and the other rich in sodium salt, appeared. However, above the eutectic temperature only the liquid phase persisted. The presence of a second Na-rich phase was also confirmed by scanning electron microscopy, X-ray diffraction and nuclear magnetic resonance. The benefit of multiple phase transitions within these OIPCs is through the increasing disorder of the lattice. This is evident within conductivity measurements that revealed that the 40 mol% NaTFSI sample at temperatures just below the eutectic temperature (i.e., solid state), shows 3 orders of magnitude higher ionic conductivity compared to that of the pure OIPC (Figure 10b). Thus demonstrating that solid-state OIPCs mixed with sodium salts can be sufficiently conductive to be applied in Na batteries.^[162]

Chimdi et al. have also considered the phase behavior, dynamics and ion conductivity of mixtures of an *N*-methyl-*N*-methylpyrrolidinium dicyanamide OIPC (C₁mpyrDCA) and sodium dicyanamide. By once again constructing a phase diagram from DSC data the authors reported that this binary system has a eutectic transition at a temperature ≈89 °C, at a composition of 20 mol% NaDCA. The conductivities in this binary system approached 0.3 S cm⁻¹ for the 50 mol% NaDCA composition just below the eutectic temperature, where the system is still solid.^[163]

4.2. Solid-State Electrolytes

The phase behavior, conductivity and electrochemical behavior of a mixture of a phosphonium cation-based OIPCs with small alkyl chain length (P₁₁₁₄[TFSI]) and NaTFSI has been investigated by Makhlooghiazad et al. recently. The detailed phase diagram was determined over the whole range of NaTFSI concentrations (0–100 mol% NaTFSI in P₁₁₁₄[TFSI]) and is shown in **Figure 11**. The phase behavior of these mixtures is complex with a eutectic transition at 36 ± 0.5 °C for the 5 mol% NaTFSI composition. A new intermediate compound at a composition of 4:1, i.e., [Na_{0.2}(P₁₁₁₄)_{0.8}][TFSI] which led to a new Na⁺ ion conductor was also explored. For compositions above 20 mol% NaTFSI a peritectic transition at 45 °C was observed. Ionic conductivity measurements revealed high ionic conductivity for the 25 mol% and 75 mol% NaTFSI compositions (Figure 11b). The high concentration of sodium salt in the latter sample means it is predominantly in the solid state. The electrochemical behavior of these two compositions (one purely in the liquid phase and the other a solid phase) to support Na electrochemistry were investigated. Stable stripping and plating of sodium in a symmetrical Na|Na cell with a high concentration of Na salt in OIPC (75 mol% of NaTFSI) at 50 and 60 °C was shown at 0.1 mA cm⁻² applying 10 min polarization steps for over 100 cycles. Cycling of half cells (Na|25 mol% NaTFSI|NaFePO₄) at 50 °C delivered stable discharge capacities of ≈76 mAh g⁻¹ at C/10 with high Coulombic efficiency. These observations indicated the possibility of using such OIPC electrolytes in sodium

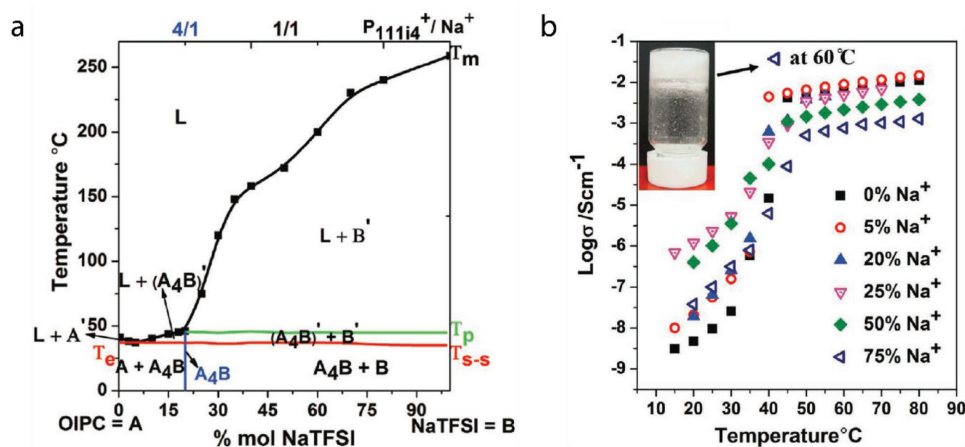


Figure 11. a) Phase diagram of P_{111i4} [TFSI] and NaTFSI binary systems. b) Ionic conductivity of P_{111i4} [TFSI] electrolytes with varying concentrations of NaTFSI. Reproduced with permission.^[164] Copyright 2016, Wiley-VCH.

devices.^[164] Electrochemical cycling of 50 mol% NaTFSI/ P_{111i4} [TFSI] has also been measured in a hybrid cell–carbon capacitor cathode and sodium metal anode,^[179] showing impressive average discharge voltage of ≈ 3 V with good stability.

Recently, the phase behavior, transport properties and electrochemical behavior of mixtures of the methyl, triisobutyl based OIPC $P_{1i4i4i4}$ [FSI] and its corresponding NaFSI salt was also reported by Makhlooghiyazad et al. Once again, these OIPCs were demonstrated as electrolytes in Na|Na symmetrical cells containing as much as 90 mol% NaFSI with very low and stable polarization potential (200 mV) at 50 and 90 °C at 0.05 and 0.1 mA cm⁻², respectively (Figure 12).^[165] The influence of size and symmetry of the cations and anions which make up these OIPCs has also been studied. Systems including NaFSI/ $P_{1i4i4i4}$ [FSI] and NaTFSI/ $P_{1i4i4i4}$ [TFSI] as well as NaTFSI/ P_{111i4} [TFSI] were directly compared to reveal that OIPCs consisting of a smaller cation and anion have superior properties in terms of lower T_m , higher conductivity and greater diffusivity of ions than their bulkier counterparts.^[180]

The effect of mixed anions has recently been explored for the $P_{1i4i4i4}$ [FSI] OIPC with the addition of either NaTFSI or NaPF₆.^[98] $P_{1i4i4i4}$ [FSI]/NaPF₆ mixtures exhibited complicated

phase behavior with a higher melting temperature, compared to that of the neat $P_{1i4i4i4}$ [FSI]. On the other hand the NaTFSI additions had a similar influence to the NaFSI such that NaFSI/ $P_{1i4i4i4}$ [FSI] and NaTFSI/ $P_{1i4i4i4}$ [FSI] showed similar phase behavior and ionic conductivity. Na|Na symmetrical cells containing either NaFSI or NaTFSI samples showed extremely stable cycling at room temperature and at 50 °C. In contrast, in order to establish a smooth and stable SEI layer in a cell with 20 mol% NaPF₆ electrolyte, a conditioning period using a higher current density or an extended time was required.^[98] Such conditioning periods to achieve more stable metal plating and stripping have been observed before for ionic liquids and superconcentrated electrolyte systems for both Li and Na.^[164,165]

5. Conclusions and Perspectives

Ionic liquids exhibit advantageous intrinsic properties and have shown promise as candidates in sodium battery applications building on progress in the lithium field. These ionic liquid electrolytes have several benefits over the conventional organic solvents borrowed from Li-ion; particularly their increased

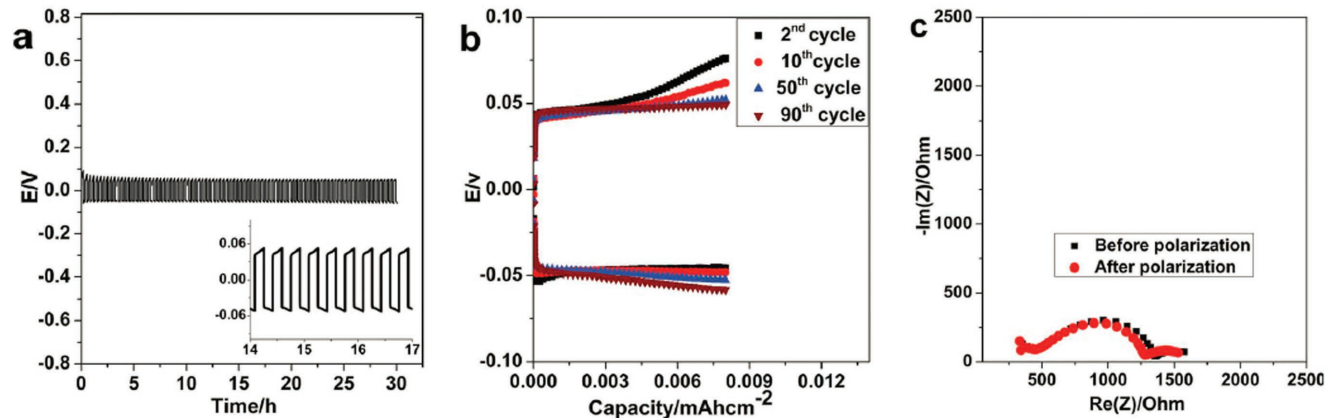


Figure 12. a,b) Galvanostatic cycling of 90 mol% NaFSI/ $P_{1i4i4i4}$ [FSI] at 50 °C using a Na⁰ metal electrode with a controlled current density of 0.05 mA cm⁻² (polarization period of 10 min) and c) associated impedance data. Reproduced with permission.^[165] Copyright 2017, Royal Society of Chemistry.

solubility to provide superconcentrated electrolytes, the great electrochemical and thermal stability range and good transport of the Na⁺ charge carrier. The flexibility in design of these novel solvents demands investigation of the properties of yet to be unveiled novel ionic liquids tailored for applications. Further functionalizing cations and anions toward improved solvation and mobility of the charge carrier is expected to bring about these developments. This has recently been reported through the investigation of organic ionic plastic crystals that are solid and don't suffer from leakage, enhance safety and still retain liquid character for the benefit of conductivity and battery performance.

A variety of electrode materials have been tested using ionic liquid electrolytes, although this number is still limited, these reports show that ionic liquid electrolytes have the potential to replace conventional solvent based electrolytes in terms of capacity, cycle stability, high temperature performance, and safety. Studies have predominantly focused on pyrrolidinium ionic liquids amassing a great deal of knowledge for this cation. These studies should be expanded to other classes of ionic liquids such as phosphonium systems and/or functionalized cations. The effect of different anions is also shown to be important, and this is an area which may be quickly unveiled, some studies have already looked into mixed anion electrolytes with a clear anion-dependence apparent for electrochemical performances. Recent work investigating how temperature, salt form and concentration affect the performance of these cells comprised of ionic liquid electrolytes reveals that this field is still growing with exciting and promising results remaining ahead.

These novel electrolytes have been characterized using classical techniques to determine their physicochemistry and thermal behavior, however the use of superconcentrated electrolytes have found that electrochemical techniques such as transport number calculation have provided keen insights. Further validating the characterization of these electrolytes using electrochemical techniques. In addition, electrochemical techniques such as impedance spectroscopy will be immensely valuable as a tool for the investigation of the electrode–electrolyte interface as it has been with Li technologies. A thorough study into the nature of the solid-electrolyte interphase is yet to be carried out for these electrolytes with the variety of electrode materials reported herein. The knowledge gained from such a study will undoubtedly provide insight for future sodium battery device applications.

In order to realize commercial sodium based batteries utilizing an ionic liquid electrolyte, a number of key hurdles must be overcome. These include the intrinsic viscosity and density of ionic liquids that can create processing and wetting issues during manufacturing, and may also lead to a drop in specific energy of a cell. Although the moderate and intermediate temperature studies of these electrolytes have shown great promise thus highlighting the limitations of conventional carbonate electrolytes in Na-ion cells, it is at lower temperatures that performance must be enhanced. The cost of these unique solvents is also an important factor in cell design and manufacture, however these are not of drastic concern in comparison to other cell components. The reports herein have shown that by increasing the salt content to be “superconcentrated” (> 50 mol%) the relative decrease in ionic liquid required will drastically reduce the

cost of an electrolyte, while still retaining and oftentimes benefiting cell performance. If favorable economy of scale for these materials can be achieved, application of these electrolytes for intermediate temperature applications appears to be a viable future technology.

Supporting Information

Supporting Information is available from the Wiley Online Library or from the author.

Acknowledgements

The authors acknowledge the ARC (Australian Research Council) for its financial support through Australian Laureate Fellowship FL110100013 (M.F.) and FL120100019 (D.R.M.), Discovery Project (DP160101178) and the ARC Centre of Excellence for Electromaterials Science (ACES, CE140100012).

Conflict of Interest

The authors declare no conflict of interest.

Keywords

advanced electrolytes, organic ionic plastic crystals, rechargeable sodium batteries, room temperature ionic liquids, sodium energy storage

Received: December 12, 2017

Revised: February 5, 2018

Published online: May 2, 2018

- [1] M. Armand, J. M. Tarascon, *Nature* **2008**, 451, 652.
- [2] J. M. Tarascon, M. Armand, *Nature* **2001**, 414, 359.
- [3] P. G. Bruce, S. A. Freunberger, L. J. Hardwick, J.-M. Tarascon, *Nat. Mater.* **2011**, 11, 19.
- [4] T. Nagaura, K. Tozawa, *Prog. Batteries Sol. Cells* **1990**, 9, 209.
- [5] J. T. Kummer, N. Weber, *SAE Trans.* **1968**, 76, 1003.
- [6] J. Coetzer, *J. Power Sources* **1986**, 18, 377.
- [7] H. Chen, T. N. Cong, W. Yang, C. Tan, Y. Li, Y. Ding, *Prog. Nat. Sci.* **2009**, 19, 291.
- [8] I. Gyuk, M. Johnson, J. Vetrano, K. Lynn, W. Parks, R. Handa, L. D. Kannberg, S. Hearne, K. Waldrip, R. Braccio, US DOE, *Grid Energy Storage*, U.S. Department of Energy, Washington, DC **2013**.
- [9] T. Tamakoshi, presented at *Fourth Int. Conf. on Sodium Batteries*, Tokyo, Japan, (accessed: November 2017).
- [10] C. Eustis, I. Gyuk, US DOE, *Energy Storage Safety Strategic Plan*, U.S. Department of Energy, Washington, DC **2014**.
- [11] B. Nykvist, M. Nilsson, *Nat. Clim. Change* **2015**, 5, 329.
- [12] M. Ati, A. Darwiche, L. Simonin, N. Martin, N. Hall, Y. Chatillon, A. Ponrouch, L. Monconduit, L. Croguennec, S. Boulinau, R. Dedryvère, C. Masquelier, M. Morcrette, P. Rozier, M. R. Palacin, J.-M. Tarascon, in *17th Int. Meeting on Lithium Batteries*, The Electrochemical Society, Como, Italy **2014**.
- [13] J. Barker, R. J. Heap, N. Roche, C. Tan, R. Sayers, J. Whitley, Y. Liu, in *2nd Int. Symp. on Sodium Batteries*, Chandler, AZ, **2015**.
- [14] P. Hartmann, C. L. Bender, J. Sann, A. K. Durr, M. Jansen, J. Janek, P. Adelhelm, *Phys. Chem. Chem. Phys.* **2013**, 15, 11661.

- [15] P. C. Howlett, D. R. MacFarlane, A. F. Hollenkamp, *Electrochim. Solid State Lett.* **2004**, 7, A97.
- [16] P. C. Howlett, D. R. MacFarlane, A. F. Hollenkamp, *J. Power Sources* **2003**, 114, 277.
- [17] N. Pylahan, M. Kerner, D. H. Lim, A. Matic, P. Johansson, *Electrochim. Acta* **2016**, 216, 24.
- [18] D. R. MacFarlane, M. Forsyth, E. I. Izgorodina, A. P. Abbott, G. Annat, K. Fraser, *Phys. Chem. Chem. Phys.* **2009**, 11, 4962.
- [19] M. Watanabe, M. L. Thomas, S. Zhang, K. Ueno, T. Yasuda, K. Dokko, *Chem. Rev.* **2017**, 117, 7190.
- [20] M. Armand, F. Endres, D. R. MacFarlane, H. Ohno, B. Scrosati, *Nat. Mater.* **2009**, 8, 621.
- [21] D. R. MacFarlane, N. Tachikawa, M. Forsyth, J. M. Pringle, P. C. Howlett, G. D. Elliott, J. H. Davis, M. Watanabe, P. Simon, C. A. Angell, *Energy Environ. Sci.* **2014**, 7, 232.
- [22] F. Endres, S. Zein El Abedin, *Phys. Chem. Chem. Phys.* **2006**, 8, 2101.
- [23] T. Welton, *Chem. Rev.* **1999**, 99, 2071.
- [24] J. M. Pringle, *Phys. Chem. Chem. Phys.* **2013**, 15, 1339.
- [25] H. Ota, K. Shima, M. Ue, J. Yamaki, *Electrochim. Acta* **2004**, 49, 565.
- [26] H. Yoon, G. H. Lane, Y. Shekibi, P. C. Howlett, M. Forsyth, A. S. Best, D. R. MacFarlane, *Energy Environ. Sci.* **2013**, 6, 979.
- [27] A. Basile, A. I. Bhatt, A. P. O'Mullane, *Nat. Commun.* **2016**, 7, 11794.
- [28] M. Forsyth, P. C. Howlett, A. E. Somers, D. R. MacFarlane, A. Basile, *Npj Mater. Degrad.* **2017**, 1, 18.
- [29] G. H. Lane, *Electrochim. Acta* **2012**, 83, 513.
- [30] P. C. Howlett, N. Brack, A. F. Hollenkamp, M. Forsyth, D. R. MacFarlane, *J. Electrochem. Soc.* **2006**, 153, A595.
- [31] D. Aurbach, E. Zinigrad, Y. Cohen, H. Teller, *Solid State Ionics* **2002**, 148, 405.
- [32] S. K. Martha, E. Markevich, V. Burgel, G. Salitra, E. Zinigrad, B. Markovsky, H. Sclar, Z. Pramovich, O. Heik, D. Aurbach, I. Exnar, H. Buqa, T. Drezen, G. Semrau, M. Schmidt, D. Kovacheva, N. Saliyski, *J. Power Sources* **2009**, 189, 288.
- [33] K. N. Wood, E. Kazayak, A. F. Chadwick, K.-H. Chen, J.-G. Zhang, K. Thornton, N. P. Dasgupta, *ACS Cent. Sci.* **2016**, 2, 790.
- [34] S. Begić, H. Li, R. Atkin, A. F. Hollenkamp, P. C. Howlett, *Phys. Chem. Chem. Phys.* **2016**, 18, 29337.
- [35] F. Endres, O. Höfft, N. Borisenko, L. H. Gasparotto, A. Prowald, R. Al-Salman, T. Carstens, R. Atkin, A. Bund, S. Zein El Abedin, *Phys. Chem. Chem. Phys.* **2010**, 12, 1724.
- [36] R. Atkin, N. Borisenko, M. Drüschler, F. Endres, R. Hayes, B. Huber, B. Roling, *J. Mol. Liq.* **2014**, 192, 44.
- [37] R. Hayes, G. G. Warr, R. Atkin, *Chem. Rev.* **2015**, 115, 6357.
- [38] A. Lewandowski, A. Swiderska-Mocek, *J. Power Sources* **2009**, 194, 601.
- [39] V. Armel, M. Forsyth, D. R. MacFarlane, J. M. Pringle, *Energy Environ. Sci.* **2011**, 4, 2234.
- [40] F. Karadas, M. Atilhan, S. Aparicio, *Energy Fuels* **2010**, 24, 5817.
- [41] F. Endres, *ChemPhysChem* **2002**, 3, 144.
- [42] J. P. Hallett, T. Welton, *Chem. Rev.* **2011**, 111, 3508.
- [43] E. L. Smith, A. P. Abbott, K. S. Ryder, *Chem. Rev.* **2014**, 114, 11060.
- [44] U. A. Rana, M. Forsyth, D. R. MacFarlane, J. M. Pringle, *Electrochim. Acta* **2012**, 84, 213.
- [45] T. L. Greaves, C. J. Drummond, *Chem. Rev.* **2008**, 108, 206.
- [46] J. Wang, Y. Yamada, K. Sodeyama, E. Watanabe, K. Takada, Y. Tateyama, A. Yamada, *Nat. Energy* **2018**, 3, 22.
- [47] J. Qian, W. A. Henderson, W. Xu, P. Bhattacharya, M. Engelhard, O. Borodin, J.-G. Zhang, *Nat. Commun.* **2015**, 6, 6362.
- [48] J. Lee, Y. Lee, J. Lee, S.-M. Lee, J.-H. Choi, H. Kim, M.-S. Kwon, K. Kang, K. T. Lee, N.-S. Choi, *ACS Appl. Mater. Interfaces* **2017**, 9, 3723.
- [49] M. Forsyth, G. M. A. Girard, A. Basile, M. Hilder, D. R. MacFarlane, F. Chen, P. C. Howlett, *Electrochim. Acta* **2016**, 220, 609.
- [50] H. Yoon, A. S. Best, M. Forsyth, D. R. MacFarlane, P. C. Howlett, *Phys. Chem. Chem. Phys.* **2015**, 17, 4656.
- [51] C.-Y. Chen, T. Kiko, T. Hosokawa, K. Matsumoto, T. Nohira, R. Hagiwara, *J. Power Sources* **2016**, 332, 51.
- [52] G. M. A. Girard, M. Hilder, D. Nucciarone, K. Whitbread, S. Zavorine, M. Moser, M. Forsyth, D. R. MacFarlane, P. C. Howlett, *J. Phys. Chem. C* **2017**, 121, 21087.
- [53] S. Aminah, M. Noor, H. Yoon, M. Forsyth, D. R. MacFarlane, *Electrochim. Acta* **2015**, 169, 376.
- [54] P. C. Howlett, J. Sunarso, Y. Shekibi, E. Wasser, L. Jin, D. R. MacFarlane, M. Forsyth, *Solid State Ionics* **2011**, 204–205, 73.
- [55] A. Fukunaga, T. Nohira, R. Hagiwara, K. Numata, E. Itani, S. Sakai, K. Nitta, S. Inazawa, *J. Power Sources* **2014**, 246, 387.
- [56] T. Yamamoto, T. Yamaguchi, T. Nohira, R. Hagiwara, A. Fukunaga, S. Sakai, K. Nitta, *Electrochemistry* **2017**, 85, 391.
- [57] T. Hosokawa, K. Matsumoto, T. Nohira, R. Hagiwara, A. Fukunaga, S. Sakai, K. Nitta, *J. Phys. Chem. C* **2016**, 120, 9628.
- [58] A. Basile, F. Makhlooghiyazad, R. Yunis, D. R. MacFarlane, M. Forsyth, P. C. Howlett, *ChemElectroChem* **2017**, 4, 986.
- [59] N. Wongittharom, C.-H. Wang, Y.-C. Wang, C.-H. Yang, J.-K. Chang, *ACS Appl. Mater. Interfaces* **2014**, 6, 17564.
- [60] P. Denholm, E. Ela, B. Kirby, M. Milligan, *The Role of Energy Storage with Renewable Electricity Generation*, Golden, CO, **2010**.
- [61] P. G. Debenedetti, H. Stiller Frank, *Nature* **2001**, 410, 259.
- [62] M. Galinski, A. Lewandowski, I. Stepniak, M. Galiński, A. Lewandowski, I. Stepniak, *Electrochim. Acta* **2006**, 51, 5567.
- [63] S. Wei, S. Choudhury, J. Xu, P. Nath, Z. Tu, L. A. Archer, *Adv. Mater.* **2017**, 29, 1605512.
- [64] S. A. M. Noor, N. C. Su, L. T. Khoo, N. S. Mohamed, A. Ahmad, M. Z. A. Yahya, H. Zhu, M. Forsyth, D. R. MacFarlane, *Electrochim. Acta* **2017**, 247, 983.
- [65] A. Basile, H. Yoon, D. R. MacFarlane, M. Forsyth, P. C. Howlett, *Electrochim. Commun.* **2016**, 71, 48.
- [66] S. A. Hashmi, M. Y. Bhat, M. K. Singh, N. T. K. Sundaram, B. P. C. Raghupathy, H. Tanaka, *J. Solid State Electrochem.* **2016**, 20, 2817.
- [67] Y. Zhao, H. Wang, G. Gao, L. Qi, *Ionics* **2013**, 19, 1595.
- [68] D. Kumar, *Solid State Ionics* **2018**, 318, 65.
- [69] D. Kumar, S. A. Hashmi, *Solid State Ionics* **2010**, 181, 416.
- [70] S. Song, M. Kotobuki, F. Zheng, C. Xu, S. V. Savilov, N. Hu, L. Lu, Y. Wang, W. D. Z. Li, *J. Mater. Chem. A* **2017**, 5, 6424.
- [71] S. Lee, S.-J. Park, S. Kim, *Res. Chem. Intermed.* **2017**, 43, 5403.
- [72] M. Egashira, T. Asai, N. Yoshimoto, M. Morita, *Electrochim. Acta* **2011**, 58, 95.
- [73] A. Boschini, P. Johansson, *Electrochim. Acta* **2016**, 211, 1006.
- [74] C. H. Wang, Y. W. Yeh, N. Wongittharom, Y. C. Wang, C. J. Tseng, S. W. Lee, W. S. Chang, J. K. Chang, *J. Power Sources* **2015**, 274, 1016.
- [75] K. Matsumoto, R. Taniki, T. Nohira, R. Hagiwara, *J. Electrochem. Soc.* **2015**, 162, A1409.
- [76] K. J. Baranyai, G. B. Deacon, D. R. MacFarlane, J. M. Pringle, J. L. Scott, *Aust. J. Chem.* **2004**, 57, 145.
- [77] D. Monti, E. Jónsson, M. R. Palacín, P. Johansson, *J. Power Sources* **2014**, 245, 630.
- [78] J. Serra Moreno, G. Maresca, S. Panero, B. Scrosati, G. B. Appetecchi, *Electrochim. Commun.* **2014**, 43, 1.
- [79] K. Matsumoto, T. Hosokawa, T. Nohira, R. Hagiwara, A. Fukunaga, K. Numata, E. Itani, S. Sakai, K. Nitta, S. Inazawa, *J. Power Sources* **2014**, 265, 36.
- [80] S. A. M. Noor, P. C. Howlett, D. R. MacFarlane, M. Forsyth, *Electrochim. Acta* **2013**, 114, 766.
- [81] H. Yoon, H. Zhu, A. Hervault, M. Armand, D. R. MacFarlane, M. Forsyth, *Phys. Chem. Chem. Phys.* **2014**, 16, 12350.
- [82] M. Hilder, M. Gras, C. R. Pope, M. Kar, D. R. MacFarlane, M. Forsyth, L. A. O'Dell, *Phys. Chem. Chem. Phys.* **2017**, 19, 17461.

- [83] C. R. Pope, M. Kar, D. R. MacFarlane, M. Armand, M. Forsyth, L. A. O'Dell, *ChemPhysChem* **2016**, 17, 3187.
- [84] C. Ding, T. Nohira, R. Hagiwara, K. Matsumoto, Y. Okamoto, A. Fukunaga, S. Sakai, K. Nitta, S. Inazawa, *J. Power Sources* **2014**, 269, 124.
- [85] G. G. Eshetu, S. Jeong, P. Pandar, A. Lecocq, G. Marlair, S. Passerini, *ChemSusChem* **2017**, 10, 3146.
- [86] T. Vogl, C. Vaalma, D. Buchholz, M. Secchiaroli, R. Marassi, S. Passerini, A. Balducci, *J. Mater. Chem. A* **2016**, 4, 10472.
- [87] A. Fukunaga, T. Nohira, Y. Kozawa, R. Hagiwara, S. Sakai, K. Nitta, S. Inazawa, *J. Power Sources* **2012**, 209, 52.
- [88] M. Forsyth, H. Yoon, F. Chen, H. Zhu, D. R. MacFarlane, M. Armand, P. C. Howlett, *J. Phys. Chem. C* **2016**, 120, 4276.
- [89] P. Kubisiak, A. Eilmes, *J. Phys. Chem. B* **2017**, 121, 9957.
- [90] T. Carstens, A. Lahiri, N. Borisenko, F. Endres, *J. Phys. Chem. C* **2016**, 120, 14736.
- [91] F. Chen, P. Howlett, M. Forsyth, *J. Phys. Chem. C* **2018**, 122, 105.
- [92] K. Matsumoto, Y. Okamoto, T. Nohira, R. Hagiwara, *J. Phys. Chem. C* **2015**, 119, 7648.
- [93] C. Ding, T. Nohira, K. Kuroda, R. Hagiwara, A. Fukunaga, S. Sakai, K. Nitta, S. Inazawa, *J. Power Sources* **2013**, 238, 296.
- [94] L. Xue, T. G. Tucker, C. A. Angell, *Adv. Energy Mater.* **2015**, 5, 1.
- [95] M. Hilder, P. C. Howlett, D. Saurel, E. Gonzalo, M. Armand, T. Rojo, D. R. MacFarlane, M. Forsyth, *J. Power Sources* **2017**, 349, 45.
- [96] T. Nohira, T. Ishibashi, R. Hagiwara, *J. Power Sources* **2012**, 205, 506.
- [97] K. Kubota, T. Nohira, T. Goto, R. Hagiwara, *Electrochem. Commun.* **2008**, 10, 1886.
- [98] F. Makhlooghiazad, R. Yunis, D. Mecerreyes, M. Armand, P. C. Howlett, M. Forsyth, *Solid State Ionics* **2017**, 312, 44.
- [99] D. R. MacFarlane, A. L. Chong, M. Forsyth, M. Kar, R. Vijayaraghavan, A. Somers, J. M. Pringle, *Faraday Discuss.* **2018**, 206, 9.
- [100] M. C. Buzzeo, C. Hardacre, R. G. Compton, *ChemPhysChem* **2006**, 7, 176.
- [101] M. Egashira, T. Tanaka, N. Yoshimoto, M. Morita, *Electrochemistry* **2012**, 80, 755.
- [102] D. Monti, A. Ponrouch, M. R. Palacin, P. Johansson, *J. Power Sources* **2016**, 324, 712.
- [103] C. V. Manohar, A. Raj, K. M. Kar, M. Forsyth, D. R. MacFarlane, S. Mitra, *Sustainable Energy & Fuels* **2018**, 2, 566.
- [104] S. Theivaprakasam, J. Wu, J. C. Pramudita, N. Sharma, D. R. MacFarlane, S. Mitra, *J. Phys. Chem. C* **2017**, 121, 15630.
- [105] D. S. Silvester, R. G. Compton, *Z. Phys. Chem.* **2006**, 220, 1247.
- [106] A. M. O'Mahony, D. S. Silvester, L. Aldous, C. Hardacre, R. G. Compton, A. M. O'Mahony, D. S. Silvester, L. Aldous, C. Hardacre, R. G. Compton, *J. Chem. Eng. Data* **2008**, 53, 2884.
- [107] S. Randström, G. B. Appetecchi, C. Lagergren, A. Moreno, S. Passerini, *Electrochim. Acta* **2007**, 53, 1837.
- [108] C. Zhao, A. M. Bond, X. Lu, *Anal. Chem.* **2012**, 84, 2784.
- [109] A. Basile, A. I. Bhatt, A. P. O'Mullane, S. K. Bhargava, *Electrochim. Acta* **2011**, 56, 2895.
- [110] A. Basile, S. A. Ferdousi, F. Makhlooghiazad, R. Yunis, M. Hilder, M. Forsyth, P. C. Howlett, *J. Power Sources* **2018**, 379, 344.
- [111] BatPaC Version 3.1, <http://www.cse.anl.gov/batpac/about.html>, (accessed: November 2017).
- [112] N. Wongtharom, T.-C. Lee, C.-H. Wang, Y.-C. Wang, J.-K. Chang, *J. Mater. Chem. A* **2014**, 2, 5655.
- [113] C. Ding, T. Nohira, R. Hagiwara, A. Fukunaga, S. Sakai, K. Nitta, *Electrochim. Acta* **2015**, 176, 344.
- [114] C. Ding, T. Nohira, A. Fukunaga, R. Hagiwara, *Electrochemistry* **2015**, 83, 91.
- [115] C.-Y. Chen, K. Matsumoto, T. Nohira, R. Hagiwara, *Electrochem. Commun.* **2014**, 45, 63.
- [116] C. Ding, T. Nohira, R. Hagiwara, *Electrochim. Acta* **2017**, 231, 412.
- [117] J. Hwang, K. Matsumoto, T. Nohira, R. Hagiwara, *Electrochemistry* **2017**, 85, 675.
- [118] C. Ding, T. Nohira, R. Hagiwara, *J. Mater. Chem. A* **2015**, 3, 20767.
- [119] C. Pozo-Gonzalo, L. R. Johnson, E. Jónsson, C. Holc, R. Kerr, D. R. MacFarlane, P. G. Bruce, P. C. Howlett, M. Forsyth, *J. Phys. Chem. C* **2017**, 121, 23307.
- [120] L. G. Chagas, D. Buchholz, L. Wu, B. Vortmann, S. Passerini, *J. Power Sources* **2014**, 247, 377.
- [121] N. Casado, M. Hilder, C. Pozo-Gonzalo, M. Forsyth, D. Mecerreyes, *ChemSusChem* **2017**, 10, 1783.
- [122] P. Meister, O. Fromm, S. Rothermel, J. Kasnatscheew, M. Winter, T. Placke, *Electrochim. Acta* **2017**, 228, 18.
- [123] T. Yamamoto, T. Nohira, R. Hagiwara, A. Fukunaga, S. Sakai, K. Nitta, S. Inazawa, *Electrochim. Acta* **2014**, 135, 60.
- [124] A. Fukunaga, T. Nohira, R. Hagiwara, K. Numata, E. Itani, S. Sakai, K. Nitta, *J. Appl. Electrochem.* **2016**, 46, 487.
- [125] C.-Y. Chen, K. Matsumoto, T. Nohira, R. Hagiwara, A. Fukunaga, S. Sakai, K. Nitta, S. Inazawa, *J. Power Sources* **2013**, 237, 52.
- [126] M. H. Han, E. Gonzalo, G. Singh, T. Rojo, *Energy Environ. Sci.* **2015**, 8, 81.
- [127] C.-Y. Chen, K. Matsumoto, T. Nohira, R. Hagiwara, Y. Orikasa, Y. Uchimoto, *J. Power Sources* **2014**, 246, 783.
- [128] C.-Y. Chen, K. Matsumoto, T. Nohira, R. Hagiwara, *J. Electrochem. Soc.* **2015**, 162, A2093.
- [129] Y. Yao, Y. Jiang, H. Yang, X. Sun, Y. Yu, *Nanoscale* **2017**, 9, 10880.
- [130] S. Aladinli, F. Bordet, K. Ahlbrecht, J. Tübke, M. Holzapfel, *Electrochim. Acta* **2017**, 231, 468.
- [131] C. Ding, T. Nohira, R. Hagiwara, *Phys. Chem. Chem. Phys.* **2016**, 18, 30770.
- [132] L. Wu, A. Moretti, D. Buchholz, S. Passerini, D. Bresser, *Electrochim. Acta* **2016**, 203, 109.
- [133] H. Usui, Y. Domi, K. Fujiwara, M. Shimizu, T. Yamamoto, T. Nohira, R. Hagiwara, H. Sakaguchi, *ACS Energy Lett.* **2017**, 2, 1139.
- [134] S. Komaba, W. Murata, T. Ishikawa, N. Yabuuchi, T. Ozeki, T. Nakayama, A. Ogata, K. Gotoh, K. Fujiwara, *Adv. Funct. Mater.* **2011**, 21, 3859.
- [135] I. Hasa, S. Passerini, J. Hassoun, *J. Power Sources* **2016**, 303, 203.
- [136] P. Hartmann, C. L. Bender, M. Vračar, A. K. Dürr, A. Garsuch, J. Janek, P. Adelhelm, *Nat. Mater.* **2012**, 12, 228.
- [137] S. Ha, J.-K. Kim, A. Choi, Y. Kim, K. T. Lee, *ChemPhysChem* **2014**, 15, 1971.
- [138] N. Zhao, X. Guo, *J. Phys. Chem. C* **2015**, 119, 25319.
- [139] C. Pozo-Gonzalo, P. C. Howlett, D. R. MacFarlane, M. Forsyth, *Electrochem. Commun.* **2017**, 74, 14.
- [140] Y. Kang, F. Liang, K. Hayashi, *Electrochim. Acta* **2016**, 218, 119.
- [141] Y. Katayama, H. Onodera, M. Yamagata, T. Miura, *J. Electrochem. Soc.* **2004**, 151, A59.
- [142] M. J. Monteiro, F. F. C. Bazito, L. J. A. Siqueira, M. C. C. Ribeiro, R. M. Torresi, *J. Phys. Chem. B* **2008**, 112, 2102.
- [143] Y. Zhang, C. Pozo-Gonzalo, *Chemical Communications* **2018**, <https://doi.org/10.1039/C8CC00595H>.
- [144] E. Peled, *J. Power Sources* **1983**, 9, 253.
- [145] S. Choudhury, S. Wei, Y. Ozhas, D. Gunceler, M. J. Zachman, Z. Tu, J. H. Shin, P. Nath, A. Agrawal, L. F. Kourkoutis, T. A. Arias, L. A. Archer, *Nat. Commun.* **2017**, 8, 898.
- [146] P. C. Howlett, T. Khoo, G. Mooketsi, J. Efthimiadis, D. R. MacFarlane, M. Forsyth, *Electrochim. Acta* **2010**, 55, 2377.
- [147] Y.-J. Kim, H. Lee, H. Noh, J. Lee, S. Kim, M.-H. Ryou, Y. M. Lee, H.-T. Kim, *ACS Appl. Mater. Interfaces* **2017**, 9, 6000.
- [148] I. A. Shkrob, T. W. Marin, S. D. Chemerisov, J. F. Wishart, *J. Phys. Chem. B* **2011**, 115, 3872.
- [149] I. A. Shkrob, T. W. Marin, Y. Zhu, D. P. Abraham, *J. Phys. Chem. C* **2014**, 118, 19661.

- [150] A. Budi, A. Basile, G. Opletal, A. F. Hollenkamp, A. S. Best, R. J. Rees, A. I. Bhatt, A. P. O'Mullane, S. P. Russo, *J. Phys. Chem. C* **2012**, 116, 19789.
- [151] C. Ding, T. Nohira, R. Hagiwara, *J. Power Sources* **2017**, 354, 10.
- [152] A. Lahiri, M. Olschewski, R. Gustus, N. Borisenko, F. Endres, *Phys. Chem. Chem. Phys.* **2016**, 18, 14782.
- [153] J. Timmermans, *J. Phys. Chem. Solids* **1961**, 18, 1.
- [154] J. N. Sherwood, *The Plastically Crystalline State: Orientationally Disordered Crystals*, John Wiley & Sons, New York, **1979**.
- [155] A. Abouimrane, Y. Abu-Lebdeh, P.-J. Alarco, M. Armand, *J. Electrochem. Soc.* **2004**, 151, A1028.
- [156] P.-J. Alarco, Y. Abu-Lebdeh, A. Abouimrane, M. Armand, *Nat. Mater.* **2004**, 3, 476.
- [157] D. R. MacFarlane, J. Huang, M. Forsyth, *Nature* **1999**, 402, 792.
- [158] Z.-B. Zhou, H. Matsumoto, *Electrochem. Commun.* **2007**, 9, 1017.
- [159] M. Anouti, L. Timperman, M. el hilali, A. Boisset, H. Galiano, *J. Phys. Chem. C* **2012**, 116, 9412.
- [160] P. Wang, Q. Dai, S. M. Zakeeruddin, M. Forsyth, D. R. MacFarlane, M. Grätzel, *J. Am. Chem. Soc.* **2004**, 126, 13590.
- [161] Q. Li, X. Chen, J. Zhao, L. Qiu, Y. Zhang, B. Sun, F. Yan, *J. Mater. Chem.* **2012**, 22, 6674.
- [162] M. Forsyth, T. Chimdi, A. Seeber, D. Gunzelmann, P. C. Howlett, *J. Mater. Chem. A* **2014**, 2, 3993.
- [163] T. Chimdi, D. Gunzelmann, J. Vongsvivut, M. Forsyth, *Solid State Ionics* **2015**, 272, 74.
- [164] F. Makhlooghiazad, D. Gunzelmann, M. Hilder, D. R. MacFarlane, M. Armand, P. C. Howlett, M. Forsyth, *Adv. Energy Mater.* **2016**, 7, 1601272.
- [165] F. Makhlooghiazad, P. C. Howlett, X. Wang, M. Hilder, D. R. MacFarlane, M. Armand, M. Forsyth, *J. Mater. Chem. A* **2017**, 5, 5770.
- [166] L. Jin, P. C. Howlett, J. M. Pringle, J. Janikowski, M. Armand, D. R. MacFarlane, M. Forsyth, *Energy Environ. Sci.* **2014**, 7, 3352.
- [167] Y. Abu-Lebdeh, P. J. Alarco, A. Abouimrane, L. Ionescu-Vasii, A. Hammami, M. Armand, *J. New Mater. Electrochem. Syst.* **2005**, 8, 197.
- [168] Y. Shekibi, A. Gray-Weale, D. R. MacFarlane, A. J. Hill, M. Forsyth, *J. Phys. Chem. C* **2007**, 111, 11463.
- [169] Y. Shekibi, S. J. Pas, N. M. Rocher, B. R. Clare, A. J. Hill, D. R. MacFarlane, M. Forsyth, *J. Mater. Chem.* **2009**, 19, 1635.
- [170] Y. Zhou, X. Wang, H. Zhu, M. Armand, M. Forsyth, G. W. Greene, J. M. Pringle, P. C. Howlett, *Phys. Chem. Chem. Phys.* **2017**, 19, 2225.
- [171] X. Wang, H. Zhu, G. W. Greene, J. Li, N. Iranipour, C. Garnier, J. Fang, M. Armand, M. Forsyth, J. M. Pringle, P. C. Howlett, *J. Mater. Chem. A* **2016**, 4, 9873.
- [172] J. Adebahr, N. Ciccotillo, Y. Shekibi, D. Macfarlane, A. Hill, M. Forsyth, *Solid State Ionics* **2006**, 177, 827.
- [173] Y. Abu-Lebdeh, A. Abouimrane, P. J. Alarco, M. Armand, *J. Power Sources* **2006**, 154, 255.
- [174] L. Jin, P. Howlett, J. Efthimiadis, M. Kar, D. Macfarlane, M. Forsyth, *J. Mater. Chem.* **2011**, 21, 10171.
- [175] P.-J. Alarco, *Solid State Ionics* **2004**, 172, 53.
- [176] W. A. Henderson, D. M. Seo, Q. Zhou, P. D. Boyle, J.-H. Shin, H. C. De Long, P. C. Trulove, S. Passerini, *Adv. Energy Mater.* **2012**, 2, 1343.
- [177] E. Cooper, C. Angell, *Solid State Ionics* **1986**, 18–19, 570.
- [178] Q. Zhou, P. D. Boyle, L. Malpezzi, A. Mele, J.-H. H. Shin, S. Passerini, W. A. Henderson, *Chem. Mater.* **2011**, 23, 4331.
- [179] M. Forsyth, M. Hilder, P. C. Howlett, F. Makhlooghiazad, D. R. MacFarlane, *WO 2017/091854 A1*, **2017**.
- [180] F. Makhlooghiazad, J. Guazzagaloppa, L. A. O'Dell, R. Yunis, A. Basile, P. C. Howlett, M. Forsyth, *Phys. Chem. Chem. Phys.* **2018**, 20, 4721.
- [181] M. Hilder, P. C. Howlett, D. Saurel, E. Gonzalo, A. Basile, M. Armand, T. Rojo, M. Kar, D. R. MacFarlane, M. Forsyth, *Electrochim. Acta* **2018**, 268, 94.
- [182] F. Wu, N. Zhu, Y. Bai, L. Liu, H. Zhou, C. Wu, *ACS Appl. Mater. Interfaces* **2016**, 8, 21381.
- [183] V. A. Nikitina, A. Nazet, T. Sonnleitner, R. Buchner, *J. Chem. Eng. Data* **2012**, 57, 3019.